LBL--28820

DE91 001797

Invited Talk Presented at:
Workshop on Beam Dynamics Issues of
High-Luminosity Asymmetric Collider Rings
Berkeley, California
February 12–16, 1990

Influence of Collective Effects on the Performance of High-Luminosity Colliders*

April, 1990

Michael S. Zisman
Exploratory Studies Group
Accelerator & Fusion Research Division
Lawrence Berkeley Laboratory
Berkeley, CA 94720

* This work was supported by the Director, Office of Energy Research, Office of High Energy and Nuclear Physics, High Energy Physics Division, U.S. Department of Energy, under Contract No. DE-AC03-76SF00098.

Influence of Collective Effects on the Performance of High-Luminosity Colliders*

Michael S. Zisman
Exploratory Studies Group
Accelerator & Fusion Research Division
Lawrence Berkeley Laboratory
Berkeley, California 94720
U.S.A.

April, 1990

Abstract

The design of a high-luminosity electron-positron collider to study B physics is a challenging task from many points of view. In this paper we consider the influence of collective effects on the machine performance; most of our findings are "generic," in the sense that they depend rather weakly on the details of the machine design. Both single-bunch and coupled-bunch instabilities are described and their effects are estimated based upon an example machine design (APIARY-IV). In addition, we examine the possibility of emittance growth from intrabeam scattering and calculate the beam lifetime from both Touschek and gas scattering. We find that the single-bunch instabilities should not lead to difficulty, and that the emittance growth is essentially negligible. At a background gas pressure of 10 nTorr, beam lifetimes of only a few hours are expected. Multibunch growth rates are very severe, even when using an optimized RF system consisting of single-cell, room-temperature RF cavities with geometrical shapes typical of superconducting cavities. Thus, a powerful feedback system will be required. In terms of collective effects, it does not appear that there are any fundamental problems standing in the way of successfully designing and building a high-luminosity B factory.

* This work was supported by the Director, Office of Energy Research, Office of High Energy and Nuclear Physics, High Energy Physics Division, U.S. Department of Energy, under Contract No. DE-AC03-76SF00098.

INTRODUCTION

There is presently a great deal of interest by the high-energy physics community in designing a facility for the production of copious quantities of B-mesons,[1] referred to as a "B factory." The ultimate purpose of such a facility is to study CP violations, as a means of investigating detailed predictions of the Standard Model. This will require a very high luminosity for the collider, in the neighborhood of $\mathcal{L} = 1 \times 10^{34}$ cm^{-2}s^{-1}. Because such a luminosity is essentially two orders of magnitude beyond currently attained values, the design of a suitable collider presents many challenges to the accelerator physics community.

For a high-luminosity collider designed as a B factory, typical beam parameters are:

- total current, $I_{tot} \approx 1$–3 A
- number of bunches, $k_B \approx 1000$
- natural emittance, $\varepsilon_0 \approx 10$–100 nm·rad
- bunch length, $\sigma_\ell \approx 1$ cm

The high currents are necessary to achieve a high collision rate. But, to avoid difficulties with the beam-beam interaction, it is necessary to adjust the number of bunches and the beam size to keep the beam-beam tune shift below a certain maximum value that will be dictated by the storage ring itself. Because of the requirements for high beam currents and many bunches, it is necessary to store the electrons and positrons in two separate rings, irrespective of whether the two beams have the same energy (symmetric collider) or different energies (asymmetric collider). This arrangement avoids the difficulty associated with many parasitic bunch crossings at locations other than the primary interaction point, and keeps the large amount of synchrotron radiation power that must be absorbed by the vacuum chamber down to manageable levels.

In this paper, we will look at those issues related to the large beam currents required to provide a high-luminosity asymmetric collider, that is, at the *collective effects* of relevance to a B factory design. The focus here is on single-ring issues, before the beams are brought into

collision. Qualitatively, the results obtained here are independent of the choice of symmetric versus asymmetric design.

A beam circulating in a storage ring interacts with its surroundings electromagnetically by inducing image currents in the walls of the vacuum chamber and other "visible" structures, such as beam position monitor electrodes, kickers, RF cavities, bellows, valves, etc. This interaction leads, in turn, to time varying electromagnetic fields that act on the beam and can give rise to instabilities. In most electron-positron colliders, single-bunch effects are the primary concern. However, different beam bunches can communicate through the narrow-band impedances in the ring, producing coupled-bunch instabilities.

Beam particles can also interact with each other or with gas molecules in the vacuum chamber, giving rise to various scattering phenomena. These include:

- intrabeam scattering (IBS), which causes emittance growth;
- Touschek scattering, which causes beam lifetime degradation; and
- gas scattering (either elastic or Bremsstrahlung), which also causes beam lifetime degradation.

We will first look at single-bunch instability thresholds and consider the growth rates of coupled-bunch instabilities. Then we will examine the possibility of emittance growth from intrabeam scattering (IBS). Finally, we will estimate beam lifetimes from Touschek scattering and gas scattering. As we will see below, the effect of the coupled-bunch instabilities is quite severe, and will likely be one of the limitations to the performance of the B factory. The results reported here were obtained with the LBL accelerator physics code ZAP.[2]

Where specific parameters are required, we use the APIARY-IV design[3] as an example. This SLAC-LBL design, which has evolved from earlier attempts[4] to produce a self-consistent B factory design, involves two equal-circumference rings in the PEP tunnel. (It is worth noting that, at this stage, we try where possible to remain faithful to known properties of the PEP ring. In particular, we take RF parameters to correspond to the presently used 353-MHz system.)

Main features of APIARY-IV include:

- initial luminosity of 3×10^{33} cm^{-2} s^{-1};
- moderate energy asymmetry (9 GeV in PEP, 3.1 GeV in the low-energy ring);
- round beams, which give a twofold (geometrical) improvement in luminosity.

Major parameters for the APIARY-IV collider are summarized in Table I.

To calculate the design luminosity, we make use of the simplified expression in Eq. (1), taken from Ref. 4:

$$L = 2.2 \times 10^{34} \xi (1 + r) \left(\frac{IE}{\beta_y^*} \right)_{1,2} \quad (\text{cm}^{-2}\ \text{s}^{-1}) \tag{1}$$

where ξ is the maximum beam-beam tune shift for both beams (and in both transverse planes), r is the beam aspect ratio (r = 0 for a flat beam, r = 1 for a round beam), I is the beam current in amperes, E is the beam energy in GeV, and β_y^* is the beta function at the interaction point (IP) in cm. The subscript in Eq. (1) refers to the fact that the ratio $(I \cdot E/\beta^*)$ can be evaluated with parameters from either beam 1 or beam 2.

Parameter choices for the low-energy ring were driven to some extent by an attempt to achieve equal damping decrements in the two rings. This feature has been shown in beam-beam simulation studies[5] to be helpful in obtaining high luminosity, and it will also aid in the injection process.

INSTABILITIES

In this section, we describe some of the instabilities that are relevant to the design of an asymmetric B factory. Numerical evaluations will be presented to indicate the seriousness of the particular effect for a typical B factory design. Before doing so, we digress briefly to define the beam impedances that drive the various instabilities.

Impedances

Beam instabilities can occur in either the longitudinal or transverse phase planes. Longitudinal instabilities are driven by voltages induced via interactions of the beam with its environment. The strength of the interaction can be characterized by the ring impedance, $Z_{\|}(\omega)$, in ohms, which is defined in Eq. (2):

$$V_{\|}(\omega) = -Z_{\|}(\omega) \cdot I_b(\omega) \tag{2}$$

where $V_{\|}(\omega)$ is the longitudinal voltage induced in the beam per turn arising from a modulation of the beam current at some particular angular frequency, $I_b(\omega)$.

Transverse instabilities arise from the transverse dipole wake field, which gives a force that increases linearly with transverse distance from the electromagnetic center of the vacuum chamber and is antisymmetric in sign about that center. The transverse impedance (in Ω/m) is defined by

$$Z_{\perp}(\omega) = \frac{-i \int_0^{2\pi R} F_{\perp}(\omega, s)\, ds}{e \Delta I_b(\omega)} \tag{3}$$

where $F_{\perp}$ is the transverse force, integrated over one turn, experienced by a charge e having transverse displacement Δ. Explicitly, $F_{\perp}$ is given by

$$F_{\perp} = e\hat{\theta}\,(E_{\theta} + B_r) + e\hat{r}\,(E_r - B_{\theta}) \quad . \tag{4}$$

In a typical storage ring, the impedance seen by the beam can be loosely characterized as being either broadband or narrow-band. As illustrated schematically in Fig. 1, sharp discontinuities in the vacuum chamber act as local sources of wake fields. These fields have a

short time duration, which means that they include many frequency components. Thus, we refer to this impedance as a broadband impedance.

For instability calculations performed in the frequency domain (e.g., with ZAP), such impedances are typically represented with a so-called Q=1 resonator, whose analytical form is given in Eq. (5) for both the longitudinal and transverse cases.

$$Z_{\parallel}^{BB}(\omega) = \frac{R_s}{\left[1 + i\left(\frac{\omega_c}{\omega} - \frac{\omega}{\omega_c}\right)\right]} \tag{5a}$$

$$Z_{\perp}^{BB}(\omega) = \left(\frac{\omega_c}{\omega}\right)\frac{R_T}{\left[1 + i\left(\frac{\omega_c}{\omega} - \frac{\omega}{\omega_c}\right)\right]} \tag{5b}$$

This representation has convenient analytical properties and exhibits qualitatively the correct behavior for the actual impedance of a storage ring. In particular, the modulus of the longitudinal impedance, $|Z_{\parallel}|$, is proportional to frequency up to a cutoff frequency, ω_c, after which it falls off as $1/\omega$ with increasing frequency. In the calculations of longitudinal instabilities described below, we make use not of $|Z_{\parallel}|$ but of the related quantity $|Z_{\parallel}/n|$, where $n \equiv \omega/\omega_0$ is the harmonic of the revolution frequency ω_0. This quantity remains essentially constant up to the cutoff frequency, beyond which it decreases as $1/\omega^2$. As can be seen from inspection of Eq. (5b), the frequency dependence of the transverse impedance follows that of $|Z_{\parallel}/n|$.

The other category of impedance-producing objects in a typical storage ring consists of cavity-like objects, represented schematically in Fig. 2. Such objects can trap electromagnetic energy and exchange it with the beam. The wake field from a cavity oscillates for a long time, and thus gives a narrow spectrum in the frequency domain. These impedances are represented in calculations as narrow-band (i.e., high-Q) resonators, as given in Eq. (6).

$$Z_{\parallel}(\omega) = \frac{R_s}{\left[1 + i\ Q\left(\frac{\omega_r}{\omega} - \frac{\omega}{\omega_r}\right)\right]} \tag{6a}$$

$$Z_{\perp}(\omega) = \left(\frac{\omega_r}{\omega}\right) \frac{R_T}{\left[1 + i\ Q\left(\frac{\omega_r}{\omega} - \frac{\omega}{\omega_r}\right)\right]} \quad . \tag{6b}$$

Typical values for Q lie in the range of 10^2–10^5, with parasitic modes of the RF cavities being closer to the upper end of the range (unless special procedures are used to de-Q them). As a result of the relatively long duration of these wake fields, trailing beam bunches feel the effects of the bunches that preceded them. The motion of the many bunches in the ring thus becomes coupled, and can become unstable for certain patterns of relative phase between bunches. This topic will be investigated later in this paper.

Longitudinal Microwave Instability

The first instability we consider is the longitudinal microwave instability, sometimes referred to as turbulent bunch lengthening. This instability, which has been seen in numerous storage rings (both proton and electron rings), is not a "fatal" instability, in the sense that it does not lead to beam loss. The instability causes an increase in both the bunch length and the momentum spread of a bunched beam, as illustrated in Fig. 3. The threshold (peak) current for the instability is given by

$$I_p = \frac{2\pi\,|\eta|\,(E/e)\,(\beta\sigma_p)^2}{\left|\frac{Z_{\parallel}}{n}\right|^{BB}_{eff}} \tag{7}$$

where $|Z_{\parallel}/n|_{eff}$ is the effective broadband impedance of the ring and $\eta = \alpha - 1/\gamma^2$ is the phase-slip factor.

We refer to an "effective" impedance here to account for the fact that the bunch samples the storage ring impedance weighted by its power spectrum, $h(\omega)$, which is the square of the Fourier spectrum of the bunch. A short bunch—one having a frequency spectrum that extends well

beyond the cutoff frequency of the broadband impedance—does not sample the broadband impedance fully, as can be seen in Fig. 4. To evaluate the effective impedance, we calculate the summation given in Eq. (8)

$$\left|\frac{Z_{\parallel}}{n}\right|_{eff}^{BB} = \frac{\left|\sum_{p=-\infty}^{\infty} h(\omega_p)\frac{Z_{\parallel}(\omega_p)}{(\omega_p/\omega)}\right|}{\sum_{p=-\infty}^{\infty} h(\omega_p)} \tag{8}$$

where

$$h(\omega_p) = \exp\left[-\left(\frac{\omega_p \sigma_\ell}{\beta c}\right)^2\right] \tag{9}$$

and $\omega_p = p\omega_0$. The result of such an calculation is shown in Fig. 5.

This reduction in effective impedance can be modeled in calculations by making use of the "SPEAR Scaling" ansatz[6] for $\sigma_\ell < b$:

$$\left|\frac{Z_{\parallel}}{n}\right|_{eff}^{BB} = \left|\frac{Z}{n}\right|_0 \left(\frac{\sigma_\ell}{b}\right)^{1.68} \tag{10}$$

where b is the chamber radius. (In terms of the discussion above, the dependence on b in Eq. (10) results from our estimate of the cutoff frequency of the broadband impedance to be $\omega_c = c/b$.) The result of the impedance roll-off for short bunches is that the bunch lengthening threshold will be increased, as shown schematically in Fig. 6. The fact that experimental dat from PEP[7] are in good agreement with the SPEAR Scaling estimates, as can be seen in Fig. 7, provides verification that the phenomenological model has some validity.

It is worth noting that the expression given in Eq. (10), which was determined phenomenologically, is in reasonable agreement with the behavior expected from a simple Q = 1

resonator. In Fig. 5 we can see that, in the short bunch length regime, the effective impedance does follow a power-law dependence. If we fit this region to determine the power law, as shown in Fig. 8, we obtain a value of about 2 (as expected for a Q = 1 resonator). However, the *measured* bunch length data correspond to a more restricted range of σ_ℓ/b, between 0.1 and 1.0. Confining the power law fit to this range, we obtain (Fig. 9) a value of 1.58, in good agreement with the SPEAR Scaling estimate.

Given that the actual broadband impedance in a storage ring is not likely to be exactly a Q = 1 resonator shape, the above argument should not be taken as a "proof" of the SPEAR Scaling law, but rather as a justification that the general trend of SPEAR Scaling—the decrease in effective impedance for short bunches—is reasonable. Obviously, the actual roll-off of the broadband impedance in any storage ring will depend on the details of the particular vacuum chamber hardware. Indeed, in modern storage rings that are specifically designed to minimize the broadband impedance it may well be that the impedance is dominated by a few discrete items, making the concept of an amorphous broadband impedance somewhat suspect.

To evaluate what happens for a typical B factory scenario, we use parameters from Table I. The bunch lengths for the high- and low-energy APIARY rings are shown in Fig. 10 as a function of RF voltage. To achieve a natural bunch length of 1 cm requires V_{RF} = 25 MV in the high-energy ring, and V_{RF} = 10 MV in the low-energy ring. Thresholds for bunch lengthening have been estimated for both rings, based on a low-frequency broadband impedance of $|Z_\parallel/n|_0$ = 1.5 Ω (i.e., half that of the present PEP ring); the results are summarized in Fig. 11. We see that, for our chosen parameters, the required current is well below threshold for both rings. In our calculations we have ignored the effect of potential-well distortion, which—for short bunches—is predicted to reduce the bunch length; this effect is estimated to be minor.

From these estimates, we conclude that there are no problems associated with the longitudinal microwave instability provided the impedance of the ring can be kept as low as 1.5 Ω. It is clear, however, that the low-energy ring could become a problem if we were envisioning considerably

fewer bunches or much higher currents than proposed for the APIARY collider.

Transverse Mode Coupling

In contrast to the longitudinal single-bunch instability discussed above, the transverse mode-coupling instability is a "fatal" instability, in the sense of leading to beam loss. The typical manifestation of this instability is a limitation on the current that can be injected into a single bunch. The instability arises because the imaginary part of the transverse broadband impedance causes frequency shifts of the synchrotron sidebands of the betatron motion. When the frequency shifts are sufficient to cause two sidebands to cross, an instability develops. For the electron case with which we are concerned, the typical situation is that the m = 0 and m = -1 synchrotron sidebands cross.

For long bunches, the dependence of the threshold (average) current scales with the storage ring parameters according to

$$I_b = \frac{4\,(E/e)\,\nu_s}{\langle \mathrm{Im}\,(Z_\perp)\,\beta_\perp \rangle\, R}\,\frac{4\sqrt{\pi}}{3}\,\sigma_\ell \qquad (11)$$

with

$$\nu_s = \frac{1}{\beta}\left[\frac{-h\eta V_{RF}\cos\phi_s}{2\pi\,(E/e)}\right]^{1/2} . \qquad (12)$$

From this scaling we see that, for the same ν_s value, the threshold current will be lower for a larger ring. It is also generally true that large rings have more impedance producing hardware, such as RF cavities, than do small rings. Note that it is the *beta-weighted* impedance that determines the threshold, so a significant gain can be made by "hiding" the devices contributing the transverse impedance in low-beta regions of the ring.

In the short-bunch regime of relevance for a B factory, the mode-coupling threshold is

expected to increase again, as illustrated in Fig. 12. The reason for this behavior is related to the roll-off of the impedance for short bunches discussed earlier for the longitudinal case: short bunches do not fully sample the broadband impedance of the ring. In Table II we show how typical B factory parameters compare with those for a PEP configuration in which the transverse mode-coupling threshold was determined[8] to be 8.4 mA. In PEP, the transverse impedance is dominated by the RF system, which consists of 120 cells. For a B factory, we envision a much-reduced RF system (having about 20 single-cell cavities), with a proportionate decrease in broadband impedance. Moreover, the smaller number of RF cells can be located in a lower beta region of the ring, so the reduction in beta-weighted transverse impedance will be even greater. Taking these factors into account, we expect an increase in threshold current of about a factor of three for the high-energy ring of a B factory. Even at its comparatively low beam energy, the low-energy ring is expected to have a higher threshold current than PEP. For the parameters of Table I, the required single-bunch currents for the high- and low-energy rings are 1.2 mA and 1.7 mA, respectively, so we have a comfortable margin.

Although we appear to be safe in terms of the RF contribution, we must take note of the other transverse impedance—especially for the low-energy ring—to make sure that it does not grow too large. In a B factory, for example, we will require complicated masking to shield the detector from both synchrotron radiation and scattered beam particles. This can contribute significantly to the transverse impedance. By way of warning, we show in Fig. 13 a prediction[9] of the mode-coupling threshold for the PEP low-emittance optics (developed for the synchrotron radiation users of the PEP ring). Although a threshold of 2.7 mA was predicted based on the supposedly well-known transverse impedance of the PEP ring, the experimental results, shown in Fig. 14, gave a lower threshold. It is likely that at least some of this discrepancy is related to additional transverse impedance associated with synchrotron radiation masks.

Coupled-bunch Instabilities

As discussed earlier, wake fields trapped in high-Q resonant objects can affect the motion of trailing bunches. If the decay time of the wake fields is long compared with the interbunch spacing (as is usually the case), the overall strength of the effect scales with the *total* current in the ring, and the instability growth rates are not very sensitive to the bunch pattern itself. The coupled-bunch motion in synchrotron phase space can be described as dipole (a = 1), quadrupole (a = 2), etc., as illustrated in Fig. 15. Longitudinal instability obviously requires some synchrotron motion, so the lowest-order longitudinal mode is the a = 1 mode. Transverse instability, in contrast, can occur even in the absence of synchrotron motion (denoted the a = 0 or "rigid dipole" mode).

In the case of a bunched beam in a storage ring, the bunch frequency line spectrum is given by

$$\begin{aligned} \omega_{\parallel}^{coh} &= (pk_B + s + a\nu_s)\,\omega_0 + \Delta\omega_{\parallel}^{coh} \\ &= \nu_p\,\omega_0 + \Delta\omega_{\parallel}^{coh} \end{aligned} \tag{13a}$$

and

$$\begin{aligned} \omega_{\perp}^{coh} &= (pk_B + s + \nu_\beta + a\nu_s)\,\omega_0 + \Delta\omega_{\perp}^{coh} \\ &= \nu_p^{\perp}\,\omega_0 + \Delta\omega_{\perp}^{coh} \end{aligned} \tag{13b}$$

where the index s = 0, 1, 2,... , k_B-1 labels the normal modes of the k_B bunches in terms of their bunch-to-bunch phase shift, i.e.,

$$\Delta\phi = 2\pi \frac{s}{k_B} \quad . \tag{14}$$

The physical meaning of the index s is illustrated for a simple case in Fig. 16, taken from Ref. 10.

The evaluation of coupled-bunch instability growth rates involves the calculation of the complex frequency shift $\Delta\omega_{\parallel}$ or $\Delta\omega_{\perp}$. In the Wang formalism,[11] the longitudinal frequency

shift is expressed as

$$\Delta\omega_{s,a}^{\parallel} = i\,\frac{I_b\,\omega_0^2\,\eta\,k_B}{2\pi\,\beta^2\,(E/e)\,\omega_s}\,\frac{(\sigma_\ell/R)^{2(a-1)}}{2^a\,(a-1)!}\,(Z_\parallel)_{eff}^{s,a} \tag{15a}$$

where

$$(Z_\parallel)_{eff}^{s,a} = \sum_{p=-\infty}^{\infty} (pk_B + s)^{2a}\,\exp\left\{-(pk_B + s)^2\,(\sigma_\ell/R)^2\right\}\left[\frac{Z_\parallel(\nu_p\omega_0)}{\nu_p}\right] . \tag{15b}$$

Transverse shifts are calculated in a similar manner with the expressions:

$$\Delta\omega_{s,a}^{\perp} = -i\,\frac{I_b\,c\,k_B}{4\pi\,(E/e)\,\nu_\beta}\,\frac{(\sigma_\ell/R)^{2a}}{2^a\,a!}\,(Z_\perp)_{eff}^{s,a} \tag{16a}$$

and

$$(Z_\perp)_{eff}^{s,a} = \sum_{p=-\infty}^{\infty} \left(pk_B + s + \nu_\beta - \frac{\xi}{\eta}\right)^{2a} \exp\left\{-\left(pk_B + s + \nu_\beta - \frac{\xi}{\eta}\right)^2 (\sigma_\ell/R)^2\right\}\left[Z_\perp\left(\nu_p^{\perp}\omega_0\right)\right] . \tag{16b}$$

The time dependence of either instability is $e^{-i\Delta\omega t}$, so the real part of $\Delta\omega$ gives the coherent frequency shift and the imaginary part gives the growth rate. It can be seen from the above expressions that the growth rate is related to the real part of the impedance itself. In the typical situation, about half of the bunch modes (index s) grow and half are damped. Even for the modes that have a positive growth rate, many will grow more slowly than the radiation damping rate, and thus will not present a problem.

To evaluate frequency shifts and instability growth rates quantitatively with Eq. (15) or Eq. (16), it is necessary to know the frequency dependent impedance $Z_\parallel(\nu_p\omega_0)$ or $Z_\perp(\nu_p\omega_0)$. In

particular, we must have information on the higher-order parasitic modes of the RF cavity. Using the representation in Eq. (6), we need to know R_s or R_T, ω_r, and Q for each parasitic mode. These values can be estimated reasonably well with electromagnetic codes such as URMEL,[12] or they can be measured in the actual cavity if it already exists.

For the case of a B factory, most designs are based on the use of many single-cell cavities to produce the required voltage. Although the cavities are all nominally identical, dimensional tolerances and temperature effects will generally conspire to move the parasitic modes to somewhat different frequencies in the different cells. The evaluation of coupled-bunch instabilities, then, requires that these different modes be considered in some way. The straightforward approach would be simply to take all the parasitic modes from the many RF cells and use them in the calculation. This probably requires some sort of statistical approach to assigning the parasitic mode frequencies, unless all cells are separately measured. The practical difficulty here is that the calculations become quite time consuming when many cells and many modes are involved.

To minimize the calculational effort—especially at the early design stage when no cavity exists—an alternative approach is to take the nominal modes from a single cell and de-Q them somewhat to represent the fact that the mode frequencies will vary from cell to cell, as illustrated in Fig. 17. The total strength of each mode, proportional to $n_{cell} \cdot R/Q$ (where n_{cell} is the number of RF cells), should be kept fixed in this approach. This de-Qing is only a calculational technique, and does not imply any actual changes in the modes themselves.

To reduce or eliminate problems with coupled-bunch instabilities, another type of de-Qing procedure, which involves physically reducing the Q of a high-order mode by means of a coupler or damping antenna, is sometimes undertaken. The helpfulness of this technique depends to some extent on where the modes land with respect to the rotation harmonics. In Fig. 18 we illustrate several cases. The lowest-frequency mode is sitting essentially at a beam rotation harmonic; de-Qing it then reduces the impedance sampled by the beam at that frequency and

would reduce the instability growth rate. In contrast, the middle mode is not initially sampled by the rotation harmonic, but after de-Qing the impedance seen by the beam is worse than it was originally, which would increase the instability growth rate. The highest frequency mode in Fig. 18 is beyond the frequency band sampled by the beam bunch, and so is essentially invisible as far as instabilities are concerned. Because the power spectrum of the beam, $h(\omega)$, extends to ever higher frequencies as the bunch get shorter, a short bunch can sample higher frequencies. This tends to produce higher growth rates for the regime of interest for a B factory. Furthermore, we expect minimal Landau damping (from synchrotron tune spread) for short bunches.

To minimize the instability growth rates ($1/\tau$), and thus the demands on the feedback system (for which the power requirement scales as $1/\tau^2$), it is best to try to eliminate the impedance at its source. One goal of a B factory design should be to try to use the minimum number of RF cells to provide the needed voltage (about 25 MV in the high-energy ring and about 10 MV in the low-energy ring for the case treated here). There are several implications of this choice:

- a high voltage per cell is needed, which means that a lot of RF power ($\approx$280 kW with the parameters considered here) must be put through the RF input window;
- the beam power lost to synchrotron radiation power must be replenished with few cells, again requiring high power through the RF input window.

As a result, an RF window power requirement of more than 500 kW arises—this has not yet been reached in an operating accelerator and will require R&D.

It is also desirable to choose RF cells with low impedance and the fewest possible number of parasitic modes. To accomplish this, it will probably be necessary to adopt a cell with a smooth shape and a large beam aperture, i.e., a geometry typical of a superconducting cavity. There are more or less suitable designs presently available at frequencies of about 350 MHz and 500 MHz; the design used for the estimates given here has only two longitudinal modes and one transverse mode trapped in the cell.

The choice of room-temperature versus superconducting cells is not completely clear. The superconducting option minimizes the overall power requirement, since power is no longer needed to generate the voltage, but it probably complicates the power input and removal, which must make a transition from a room-temperature to a cryogenic environment. It is also worth noting that there is presently no operating experience with superconducting RF in the high-current regime of interest to a B factory.

To get a feeling for the seriousness of the coupled-bunch instabilities, calculations have been performed for typical B factory parameters. For these calculations, it was assumed that 20 single-cell cavities for the high-energy ring and 10 such cavities for the low-energy ring were used. Other relevant parameters can be found in Table I. Two sets of calculations were performed for each ring, the first taking the nominal parasitic mode Q values generated by URMEL, and the second assuming a reduction in Q by a factor of 200. The results for the fastest growing unstable modes are summarized in Tables III and IV for the high- and low-energy ring, respectively.

The calculations predict rapid growth for the lowest synchrotron mode both longitudinally (a = 1) and transversely (a = 0). Because the rates are well beyond the radiation damping rate, a powerful feedback system is clearly needed. Moderately rapid growth is also predicted for the next higher synchrotron mode (a = 2 longitudinally; a = 1 transversely) in the case where the cavity modes are not de-Qed. However, de-Qing by a factor of 200 reduces the predicted growth rates to values comparable to or below the radiation damping rate. From the results in Tables III and IV, it appears that the benefits of de-Qing are stronger in the longitudinal than in the transverse plane. It is not clear, however, that this result can be generalized to other cases.

It is worth noting one other feature of the calculations that depends on the ring size. The 2200-m circumference assumed here corresponds to a revolution frequency of only 136 kHz. This means that the individual bunch harmonic lines are quite close together (equivalent to Q ≈ 5000 at a typical frequency of 750 MHz), making it difficult to avoid *any* parasitic modes.

SCATTERING PROCESSES

In this section, we will describe the various scattering processes that can occur, including intrabeam scattering (IBS), Touschek scattering, and gas scattering. The first of these can cause a blowup of the beam emittance, whereas the latter two effects cause a loss of particles and thus degrade the beam lifetime.

Intrabeam Scattering

The emittance growth due to IBS is a result of multiple, small-angle Coulomb scattering within a beam bunch. The collision probability is inversely proportional to the phase-space volume density of the bunch:[13]

$$g_{IBS} \propto \frac{1}{\Gamma} = \frac{1}{(2\pi \beta\gamma m_e)^3 \varepsilon_x \varepsilon_y \sigma_\ell \sigma_p} \tag{17}$$

which means that the B factory requirement for short bunches is a disadvantage. As a result of the collision, there is an exchange of energy among the three phase planes. In the bunch rest frame, the particle motion is treated nonrelativistically. Because of the distribution of particle momenta, collisions can occur. The rms momentum spreads in the three phase planes are given by

$$\text{H: } \sigma_{x'} p_0 \tag{18a}$$

$$\text{V: } \sigma_{y'} p_0 \tag{18b}$$

$$\text{L: } \frac{\sigma_p p_0}{\gamma} \quad . \tag{18c}$$

In general, the scattering event will transfer momentum from the transverse to the longitudinal

plane. However, in dispersive regions of the lattice, the change in longitudinal momentum excites a horizontal betatron oscillation because of the change in the closed orbit for the off-momentum particles, that is

$$x \rightarrow x - D_x\left(\frac{\delta p}{p}\right) \tag{19a}$$

$$x' \rightarrow x' - D'_x\left(\frac{\delta p}{p}\right) \quad . \tag{19b}$$

The measure of the emittance growth is

$$\mathcal{H} = \left[\gamma_x D^2 + 2\alpha_x DD' + \beta_x D'^2\right] \quad . \tag{20}$$

This is the same parameter as for quantum excitation, which determines the natural emittance of the lattice. One distinction between the IBS process and quantum excitation, however, is that the former can occur anywhere in the lattice, that is, it is not restricted only to the dipoles. To evaluate the equilibrium emittance, we add an additional growth term, g_{IBS}, to the standard expression that includes only radiation damping and quantum excitation:

$$\left[g_{IBS}(\varepsilon) - g_{SR}\right]\varepsilon + g_{SR}\,\varepsilon_0 = 0 \tag{21}$$

where

$$g \equiv \frac{1}{\varepsilon}\frac{d\varepsilon}{dt} \quad . \tag{22}$$

This equation is transcendental, since g_{IBS} is a function of the emittance. Nonetheless, it is possible with ZAP to calculate the IBS growth rate at many lattice points around the ring and obtain a weighted average value of g_{IBS} that can be used to solve Eq. (21). In Fig. 19 we present typical results for the B factory parameter regime, taken from Ref. 14. We see that there is no

significant emittance growth for either ring. This has, up to now, been true in all cases examined, so IBS emittance growth is not expected to be a significant problem for a B factory.

Touschek Scattering

Touschek scattering is also an intrabeam scattering process but, in contrast to the IBS multiple scattering process described above, it involves large-angle single Coulomb scattering events. In these (relatively rare) events, the momentum deviation of the scattered particle can exceed the acceptance of the storage ring. The momentum acceptance limit can come from either the longitudinal or the transverse plane.

In the longitudinal plane, there is a limit on the momentum deviation at which a particle can still undergo stable synchrotron oscillations. This is referred to as the RF acceptance (or "bucket height"), given by:

$$\left(\frac{\Delta p}{p}\right)_{bucket} = \frac{1}{\beta}\left\{\frac{-V_{RF}\left[\frac{2}{\pi}\cos\phi_s - \left(1-\frac{2}{\pi}\phi_s\right)\sin\phi_s\right]}{h\,\eta\,(E/e)}\right\}^{1/2} \tag{23}$$

where V_{RF} is the RF voltage, ϕ_s is the synchronous phase, and h is the harmonic number.

In the transverse plane, the limitation arises because, in dispersive regions of the lattice, the change in momentum excites a large betatron oscillation at the scattering location. At any other lattice location (denoted i), the maximum particle amplitude resulting from the original Touschek event is

$$\Delta x_i = \left[|D_i| + \sqrt{\beta_i\,\mathcal{H}_s}\right]\left(\frac{\delta p}{p}\right) \tag{24}$$

where $\mathcal{H}_s$ represents the function defined in Eq. (20), evaluated at the scattering location. Touschek scattered particles can thus hit the vacuum chamber wall or exceed the dynamic

aperture of the ring. For a high-luminosity collider with low-beta optics, the latter possibility is a real concern. It is important to note that, in addition to a large betatron amplitude, the scattered particles are also far off momentum—in general a bad combination. To properly assess the dynamic aperture limitation, it is necessary to track the off-momentum particles (including synchrotron oscillations and the full lattice nonlinearities).

The Touschek lifetime is a very strong function of the momentum acceptance, scaling roughly as

$$\tau_T \propto \left(\frac{\Delta p}{p}\right)^3 \tag{25}$$

so the battle for Touschek lifetime is won or lost here. The lifetime also scales inversely with the bunch volume

$$V_B \propto 8\pi^{3/2}\,\sigma_x\,\sigma_y\,\sigma_\ell \tag{26}$$

so a large bunch is helpful in this regard.

Estimates of the momentum acceptance for typical B factory parameters are shown in Fig. 20. For both the high- and low-energy rings, the acceptance is expected to be limited transversely. (The RF acceptances are unnecessarily large because the voltages are chosen to be high to maintain short bunches. In principle, the "extra" voltage is not good for the lifetime, as it serves only to decrease the bunch volume, but this is the price we must pay for short bunches.) Fortunately, the Touschek lifetime is predicted not to be a problem in this parameter regime, as demonstrated in Fig. 21. At the nominal operating energies of 9 GeV and 3.1 GeV, the Touschek lifetimes for the parameters of Ref. 14 are 400 hours and 100 hours, respectively.

Gas Scattering

Another limitation on the beam lifetime arises from interactions between electrons and residual gas atoms in the vacuum chamber. The collisions can be either elastic or inelastic (referred to as Bremsstrahlung), and both processes are important. As the electron beam energy increases, the elastic process becomes progressively less important compared with the Bremsstrahlung, so the latter typically dominates the lifetime in high-energy storage rings.

In the elastic scattering case, the electron undergoes a single Coulomb scattering that changes its angle sufficiently that it either hits the chamber wall or becomes dynamically unstable. In the ring, the motion of a particle is defined by an invariant phase-space area ("emittance") given by

$$\varepsilon_z = \frac{1 + \alpha(s)^2}{\beta(s)} z^2 + 2\alpha(s)\, z{\cdot}z' + \beta(s)\, z'^2 \tag{27}$$

where z represents either the x or y coordinate. If the z' from the scattering is too large, the emittance exceeds the acceptance of the lattice, and the scattered particle is lost somewhere in the ring. The physical acceptance is defined as

$$A_\perp = \min\left(\frac{b^2}{\beta_\perp}\right) \tag{28}$$

i.e., the smallest value in each transverse plane of the invariant emittance corresponding to a chamber half-aperture b. For a uniform chamber aperture, the acceptance limit will occur at the maximum beta function, but this is usually not the case in an actual ring. To derive the loss probability, we integrate over the Rutherford cross section and obtain[15]

$$\sigma_{el} = \frac{2\pi\, r_e^2\, Z^2}{\gamma^2} \frac{\langle \beta_\perp \rangle}{A_\perp} \tag{29}$$

where the brackets denote an average over the ring circumference.

In the case of Bremsstrahlung interactions, the inelastic scattering leads to an energy loss for the scattered particle. If the resultant momentum deviation, $\delta p/p$, exceeds the acceptance of the ring, the particle is lost. As discussed for Touschek scattering, the momentum acceptance can be limited either longitudinally or transversely. For the B factory parameters considered here, the limit is transverse. The loss probability, obtained by integrating over energy loss, is given by[15]

$$\sigma_{Br} = \frac{4}{3}\frac{4\,r_e^2\,Z^2}{137}\,ln\left(\frac{183}{Z^{1/3}}\right)\left[\,ln\left(\frac{1}{(\Delta p/p)_{lim}} - \frac{5}{8}\right)\right] . \tag{30}$$

The combined loss rate for the two gas scattering processes is given by[15]

$$\frac{1}{\tau_g} \equiv \frac{1}{N_b}\frac{dN_b}{dt} = 3.22\times 10^{22}\, n_Z\, P\, \beta c\left(\sigma_{el} + \sigma_{Br}\right) \tag{31}$$

where n_Z is the number of atoms of species Z per molecule, and P is the pressure in Torr.

To mitigate the effects of gas scattering, there are several options:

- make the apertures large;
- keep the beta functions low;
- increase the momentum acceptance;
- maintain a low residual gas pressure in the ring, especially for high-Z species.

The first option is straightforward, but is always costly because magnet aperture is expensive. Low beta functions serve to minimize the emittance increase of a scattered particle (see Eq. (27)) and to increase the acceptance of the ring for a given aperture (see Eq. (28)). From Eq. (30), we can see that the momentum acceptance has a relatively weak (logarithmic) influence on the lifetime, so improving it has little beneficial effect. The requirement for a low gas pressure is obvious, but is not so easily achieved in a ring that must accommodate up to 3 A of beam

current. Present rings operate with average pressures of about 10 nTorr (N_2-equivalent), which we take here to be an achievable, though difficult, goal.

At a pressure of 10 nTorr, the beam lifetimes from gas scattering are about 3 hours in either the high- or the low-energy ring, as summarized in Table V.

SUMMARY

In this paper we have examined the important collective effects influencing the performance of high-intensity storage rings of the type required to serve as a B factory. To achieve a high luminosity, it appears inevitable that many bunches will be used in each ring. This permits the parameters to be chosen in such a way as to minimize any possible difficulties with single-bunch effects. On the other hand, the coupled-bunch instabilities are severe and are likely to be the main performance-limiting feature of a B factory. It is likely that the success of such a collider will depend rather strongly on the skills of the feedback system designer.

The limitation on the total current that can be stored in the collider rings will come from one or more of the following:

- total synchrotron radiation power into the vacuum chamber walls;
- tolerable background gas pressure in the ring;
- coupled-bunch instability growth rates.

All of these issues are, in a sense, technology rather than physics constraints. The synchrotron radiation power can, in principle, be handled by proper design of the vacuum chamber and its cooling system. Designs to handle a linear power density of 20 kW/m appear to be practical, and this is sufficient for the typical B factory parameter regime. The second issue becomes ultimately one of pumping speed per meter of ring circumference. To maintain a pressure of 10 nTorr in the face of 3 A of circulating beam requires a pumping speed on the order of 1000 ℓ/s per meter. Achieving this is possible, but will require careful attention to the design. In terms of the coupled-bunch instabilities, the main questions concern how much the rates can be reduced by

proper design of the RF cavities, and how much growth rate can be handled by a feedback system. It seems possible, based on present technology, to reduce the instability growth rates to below 1000 s^{-1}, a rate that can be handled with a feedback system of reasonable power (a few kW). Because the feedback power requirement scales as the square of the growth rate that must be damped, however, a growth rate of 10^4 s^{-1} may be unmanageable.

For the parameter regime presently being contemplated in most B factory designs, single-bunch limitations will come mainly from the beam-beam interaction. This situation results from a conscious choice to push the instability problems into the multibunch arena, rather than picking an in-between regime in which both single- and coupled-bunch instabilities are severe. Based on the experience at existing rings, it should be possible to maintain the longitudinal impedance to a level of $|Z/n| \approx 1\ \Omega$, which will not lead to problems for the short bunches required for a B factory. Even if the impedance were somewhat higher, the bunch lengthening would probably not be a major problem. The one possible concern is that the low-energy ring is vulnerable to the transverse mode-coupling instability if the transverse impedance gets too large. It is nontrivial to minimize the impedance contribution from the many masks that will be needed to protect the detector region from synchrotron radiation and scattered particle backgrounds. In our favor, of course, is the fact that we are concerned with the beta-weighted transverse impedance, and the beta functions in this region are reasonably low.

Because the coupled-bunch instability growth rates scale with the total current and are essentially independent of the bunch pattern, the limit on the number of bunches is really dictated by the ability to separate the closely spaced bunches near the IP. A secondary issue is the bandwidth of the feedback system; this, however, is not believed to be a strong constraint on the design.

Beam lifetimes will be typical of modern colliders—on the order of a few hours—provided an adequate vacuum system can be designed. There is no reason to believe that solutions cannot be found, although they may be rather costly.

Thus, it seems fair to conclude that, in terms of collective effects, nothing yet seems to preclude the possibility of building a successful high-luminosity B factory.

ACKNOWLEDGMENTS

It is a pleasure to thank A. Garren and M. Donald for providing the lattices used in this study, and S. Chattopadhyay, Y. Chin, W. Davies-White, A. Hutton, G. Lambertson and P. Oddone for many beneficial discussions on B factory design.

REFERENCES

1. See, e.g., "Proposal for an Electron Positron Collider for Heavy Flavour Particle Physics and Synchrotron Radiation," Paul Scherrer Institute Report PR-88-09, July, 1988; "The Physics Program of a High-Luminosity Asymmetric B Factory at SLAC," Stanford Linear Accelerator Center Report SLAC-353, Lawrence Berkeley Laboratory Report LBL-27856, California Institute of Technology Report CALT-68-1588, October, 1989; A.N. Dubrovin, A.N. Skrinsky, G.N. Tumaiki, and A.A. Zholents, "Conceptual Design of a Ring Beauty Factory," European Particle Accelerator Conference, Rome, June, 1988, p. 467; H. Nesemann, W. Schmidt-Parzefall, and F. Willeke, "The Use of PETRA as a B Factory," European Particle Accelerator Conference, Rome, June, 1988, p. 439.

2. M.S. Zisman, S. Chattopadhyay, and J.J. Bisognano, "ZAP User's Manual," Lawrence Berkeley Laboratory Report LBL-21270, December, 1986.

3. "Investigation of an Asymmetric B Factory in the PEP Tunnel," Lawrence Berkeley Laboratory Report LBL PUB-5263, Stanford Linear Accelerator Center Report SLAC-359, California Institute of Technology Report CALT-68-1622, March, 1990.

4. A.A. Garren, *et al.*, "An Asymmetric B-meson Factory at PEP," in Proc. of the Particle Accelerator Conf., Chicago, March, 1989, p. 1847; "Feasibility Study for an Asymmetric B Factory Based on PEP," Lawrence Berkeley Laboratory Report LBL PUB-5244, Stanford Linear Accelerator Center Report SLAC-352, California Institute of Technology Report CALT-68-1589, October, 1989.

5. Y.H. Chin, "Beam-Beam Interaction in an Asymmetric Collider for B Physics," Lawrence Berkeley Laboratory Report LBL-27665, August, 1989, Proc. of XIV Intl. Conf. on High Energy Accelerators, to be published.

6. A.W. Chao and J. Gareyte, "Scaling Law for Bunch Lengthening in SPEAR-II," Stanford Linear Accelerator Center Note SPEAR-197, PEP-224, December, 1976.

7. M. Donald, *et al.*, "Feedback Experiment at PEP," CERN Report LEP-553, January, 1986.

8. L. Rivkin, "Collective Effects in PEP," in Proc. of Workshop on PEP as a Synchrotron Radiation Source, October 20–21, 1987, p. 139.

9. M.S. Zisman, "Collective Effects in the PEP Low-Emittance Configuration," in Proc. of Workshop on Accelerator Physics Issues Relating to the Use of PEP as a Synchrotron Radiation Source, Stanford Synchrotron Radiation Laboratory Report 88/06, November, 1988.

10. A.W. Chao, "Coherent Instabilities of a Relativistic Bunched Beam," in Physics of High Energy Particle Accelerators, American Institute of Physics Conf. Proc. 105, 1983, p. 353.

11. J.M. Wang, "Longitudinal Symmetric Coupled Bunch Modes," Brookhaven National Laboratory Report BNL-51302, December, 1980; S. Chattopadhyay and J.M. Wang, unpublished note (1986).

12. T. Weiland, "On the Computation of Resonant Modes in Cylindrically Symmetric Cavities," Nucl. Instr. and Meth. 216, 329 (1983).

13. J. Bjorken and S.K. Mtingwa, Part. Accel. 13, 115 (1983).

14. M.S. Zisman, "Study of Collective Effects for the APIARY Collider," Lawrence Berkeley Laboratory Report LBL-27676, October, 1989; Proc. of Workshop on B-Factories and Related Physics Issues, Blois, June 26 – July 1, 1989, to be published.

15. J. LeDuff, "Current and Density Limitations in Existing Electron Storage Rings," Nucl. Instr. and Meth. A239, 83 (1985).

Table I

APIARY-IV Major Parameters

	High-energy	Low-energy
Energy, E [GeV]	9	3.1
Circumference, C [m]	2200	2200
Number of bunches, k_B	1296	1296
Particles per bunch, N_B [10^{10}]	5.44	7.88
Total current, I [A]	1.54	2.23
Emittance,[a] ε_x [nm-rad]	33	66
Bunch length, σ_ℓ [mm]	10	10
Relative momentum spread, σ_p [10^{-4}]	6.1	9.5
Damping time		
$\tau_{x,y}$ [ms]	37.0	32.3
τ_E [ms]	18.5	17.3
Beta functions at IP		
β_x^* [cm]	6	3
β_y^* [cm]	6	3
Betatron tune		
horizontal, ν_x	21.28	37.76
vertical, ν_y	18.20	35.79
Synchrotron tune, Q_s	0.053	0.039
Momentum compaction, α	0.00245	0.00115
RF parameters		
frequency, f_{RF} [MHz]	353.2	353.2
voltage, V_{RF} [MV]	25	10
Nominal beam-beam tune shift		
ξ_{0x}	0.03	0.03
ξ_{0y}	0.03	0.03
Luminosity, $\mathcal{L}$ [cm^{-2} s^{-1}]	3×10^{33}	

[a]Equal horizontal and vertical emittances.

Table II

Transverse Mode-Coupling Threshold Scaling

	Low-energy	PEP	High-energy
E [GeV]	3.1	14.5	9.0
$\beta_\perp$ [m]	20	87	40
R [m]	350	350	350
Q_s [10^{-2}]	3.9	4.6	5.3
$Z_\perp$ [MΩ/m]	0.4	0.8	0.4
Relative factor[a]	1.6	1	3.1
Observed threshold [mA]	—	8.4	—

[a]Scaling factor is $F = (E\, Q_s/\beta_\perp Z_\perp R)$.

Table III

Coupled-Bunch Growth Rates for APIARY-IV

High-Energy Ring

(9 GeV; τ_E = 18.5 ms; τ_x = 37 ms)

Longitudinal

no de-Q		Q/200	
$\tau_{a=1}$ (ms)	$\tau_{a=2}$ (ms)	$\tau_{a=1}$ (ms)	$\tau_{a=2}$ (ms)
0.4	22	4	390

Transverse

no de-Q		Q/200	
$\tau_{a=0}$ (ms)	$\tau_{a=1}$ (ms)	$\tau_{a=0}$ (ms)	$\tau_{a=1}$ (ms)
1.2	38	2	66

Table IV

Coupled-Bunch Growth Rates for APIARY-IV

Low-Energy Ring

(3.1 GeV; τ_E = 17.3 ms; τ_x = 32.3 ms)

Longitudinal

no de-Q		Q/200	
$\tau_{a=1}$ (ms)	$\tau_{a=2}$ (ms)	$\tau_{a=1}$ (ms)	$\tau_{a=2}$ (ms)
0.3	20	3	290

Transverse

no de-Q		Q/200	
$\tau_{a=0}$ (ms)	$\tau_{a=1}$ (ms)	$\tau_{a=0}$ (ms)	$\tau_{a=1}$ (ms)
1	57	0.5	110

Table V

Gas Scattering Lifetimes

(P = 10 nTorr, N_2-equivalent)

	Low-energy	High-energy
Elastic [h]	10	8
Bremsstrahlung [h]	5	5
Total [h]	3	3

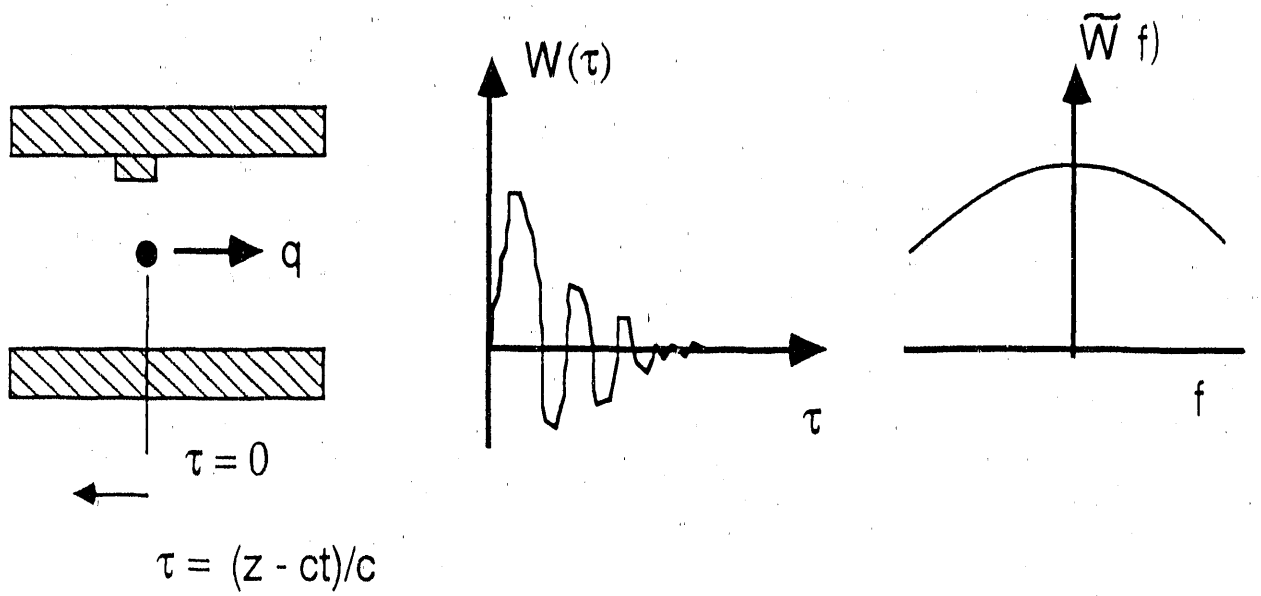

Fig. 1. Impedance properties of a sharp discontinuity in a storage ring vacuum chamber.

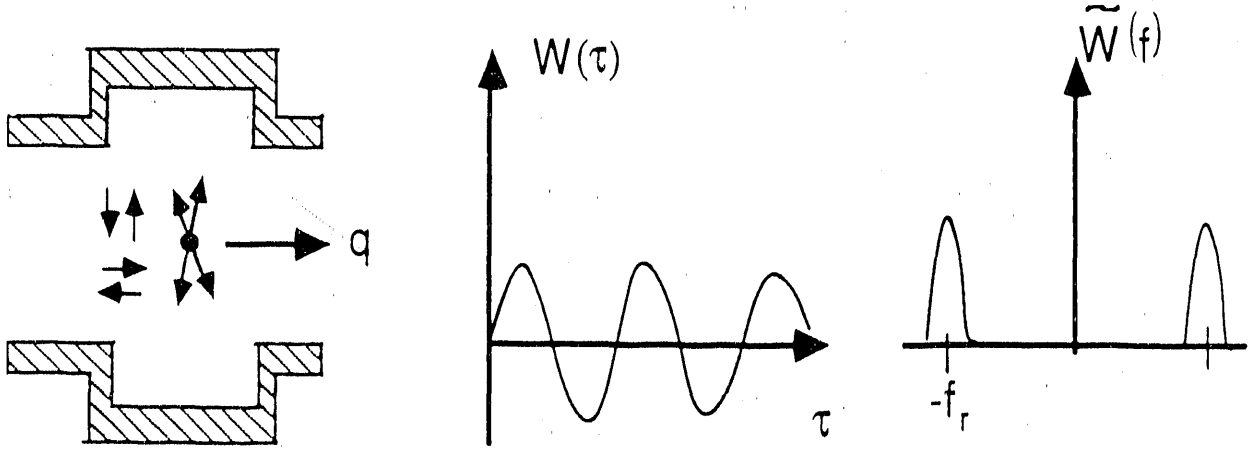

Fig. 2. Impedance properties of a cavity-like object in a storage ring vacuum chamber.

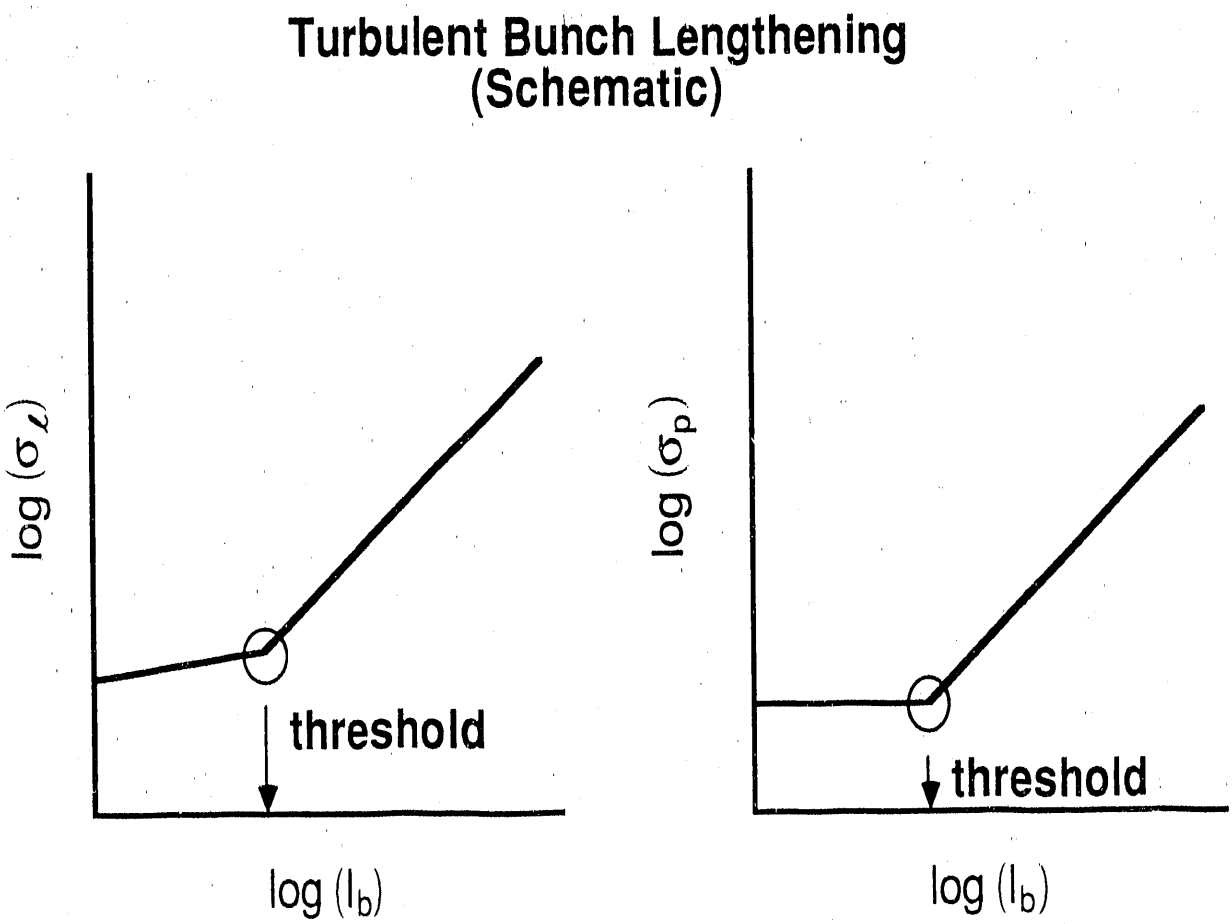

Fig. 3. Schematic of bunch lengthening and widening due to the longitudinal microwave instability.

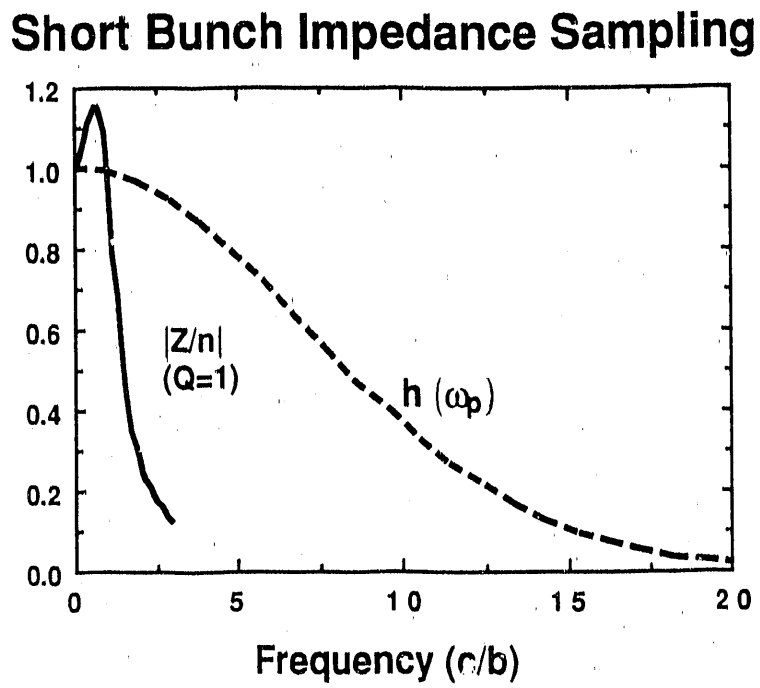

Fig. 4. Sampling of broadband impedance with short bunches.

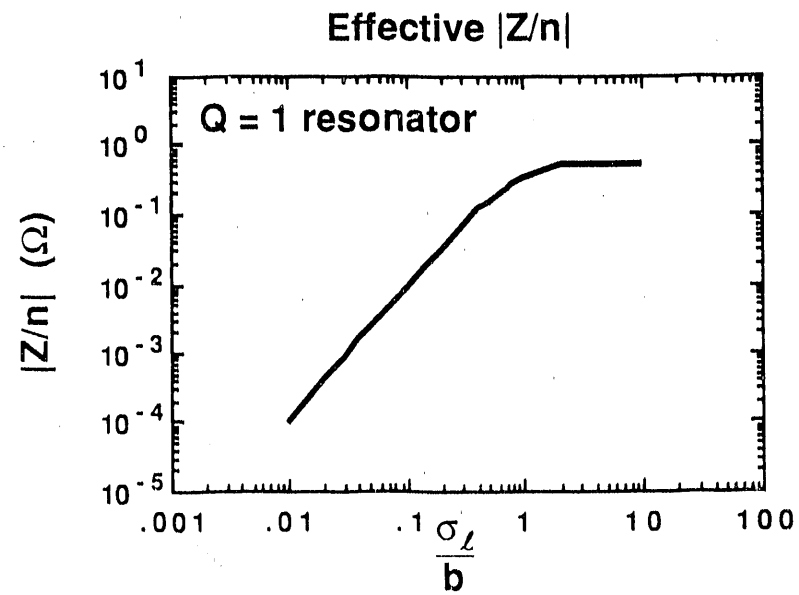

Fig. 5. Effective broadband impedance, as a function of bunch length, for a Q = 1 broadband resonator model.

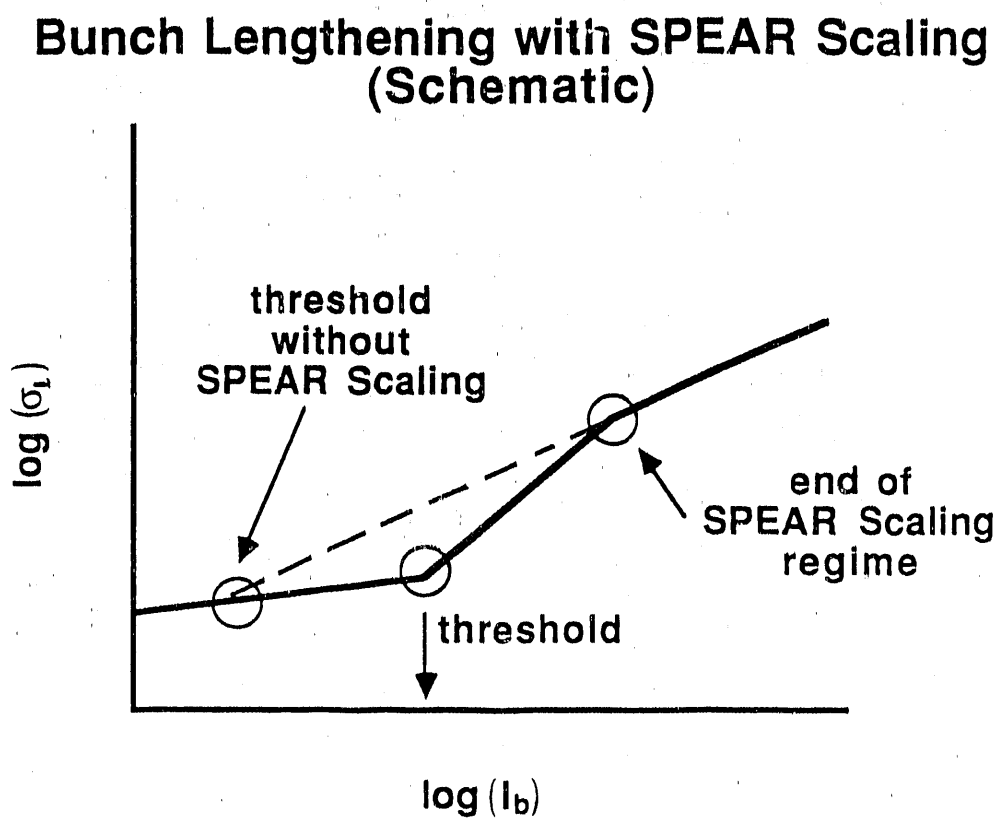

Fig. 6. Expected change in bunch lengthening behavior in the short-bunch regime.

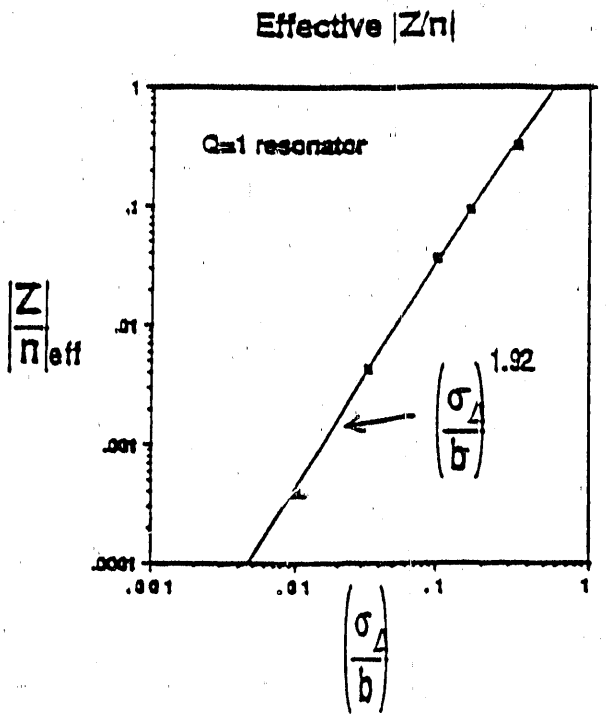

Fig. 8. Power law fit to short bunch effective impedance calculation from Fig. 5.

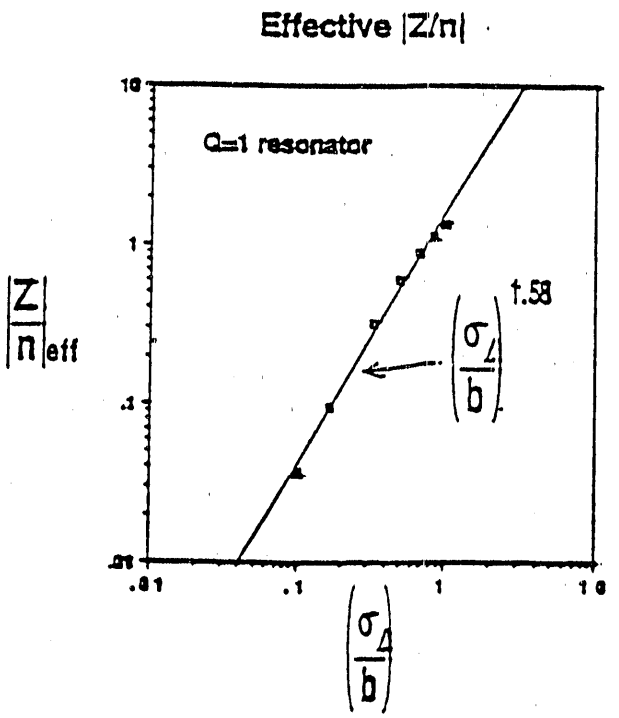

Fig. 9. Power law fit to short bunch effective impedance calculation from Fig. 5 for the restricted bunch length range $0.1 \leq \sigma_z/b \leq 1$ from which the SPEAR Scaling phenomenology was originally derived. The resultant power law is in reasonably close agreement with the value of 1.68 determined experimentally.

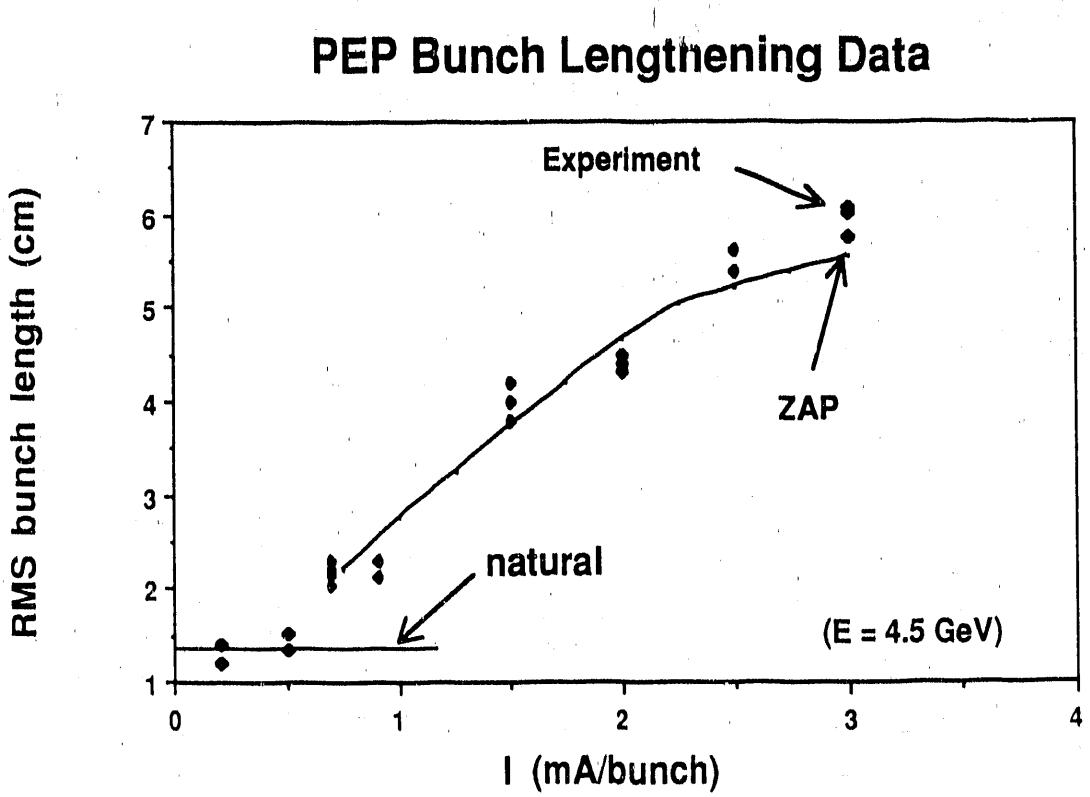

Fig. 7. Comparison of PEP bunch length measurements at 4.5 GeV with predictions based on SPEAR Scaling.

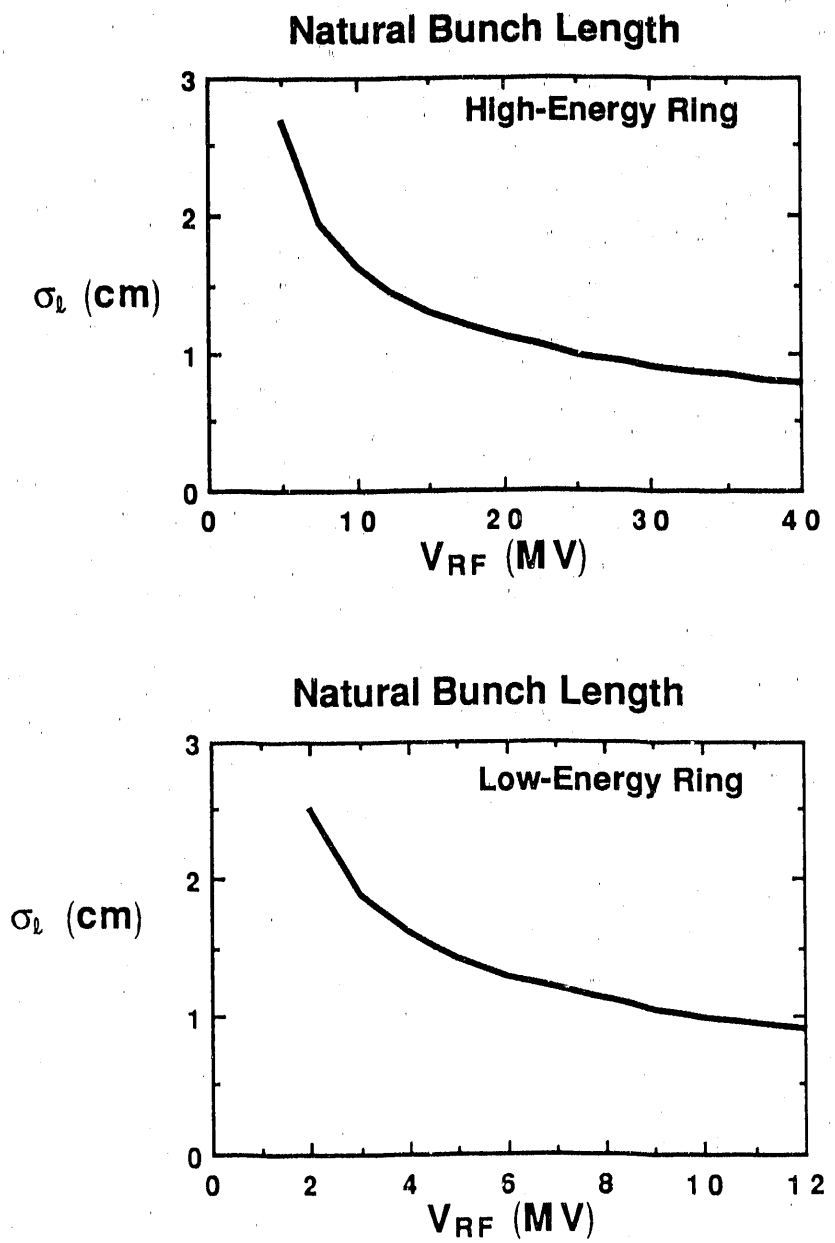

Fig. 10. Natural bunch lengths for the high-energy and low-energy APIARY-IV storage rings as a function of RF voltage.

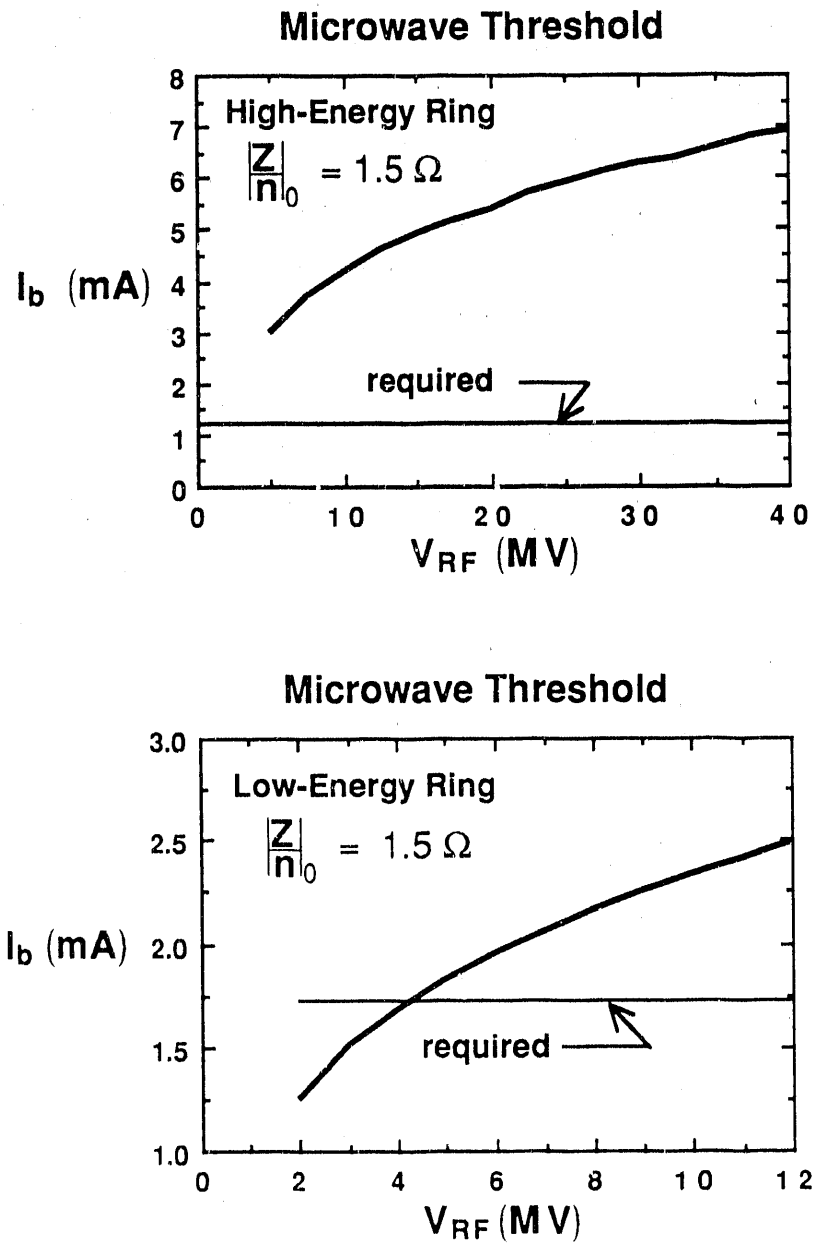

Fig. 11. Bunch lengthening thresholds for the high-energy and low-energy APIARY-IV storage rings as a function of RF voltage.

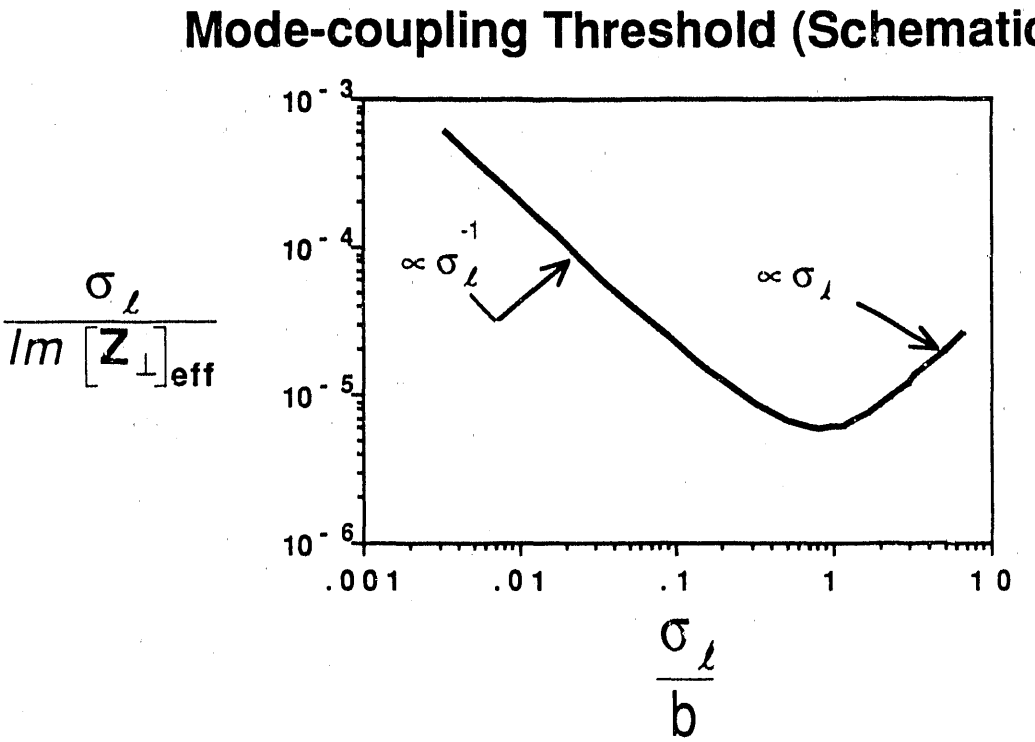

Fig. 12. Expected behavior of transverse mode-coupling threshold as a function of bunch length. In the short bunch length regime, the threshold is expected to increase because the broadband impedance is not sampled fully.

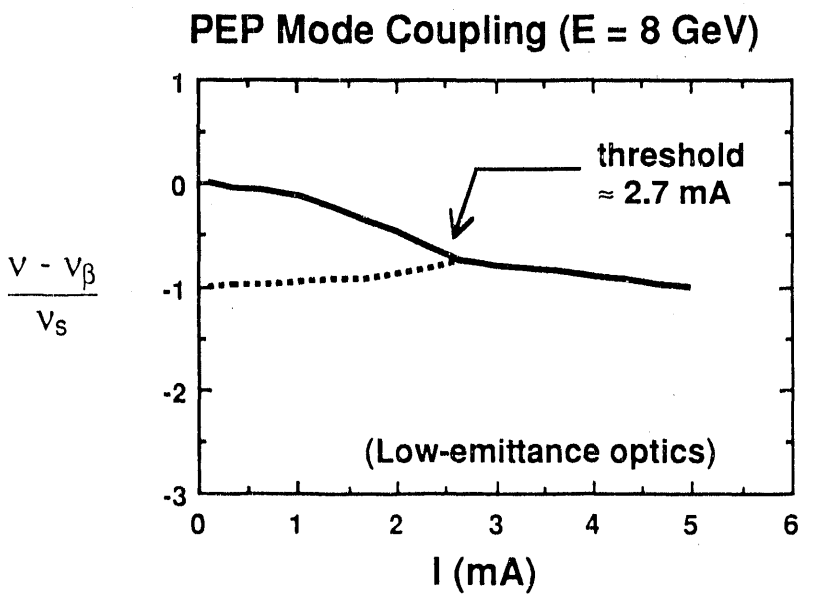

Fig. 13. Predicted mode-coupling threshold for the PEP low-emittance optics. The m = 0 and m = -1 modes cross at 2.7 mA.

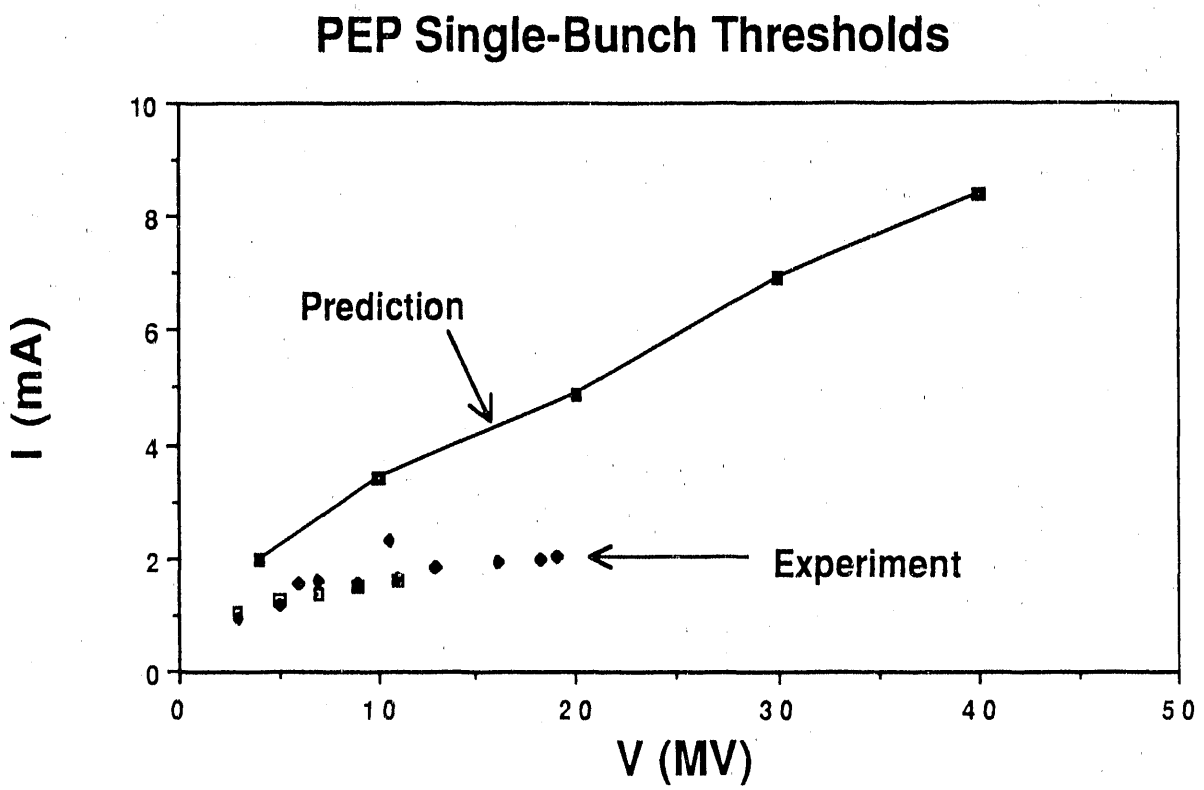

Fig. 14. Comparison between predicted mode-coupling threshold for the PEP low-emittance optics and experimental results.

Coupled-bunch Modes

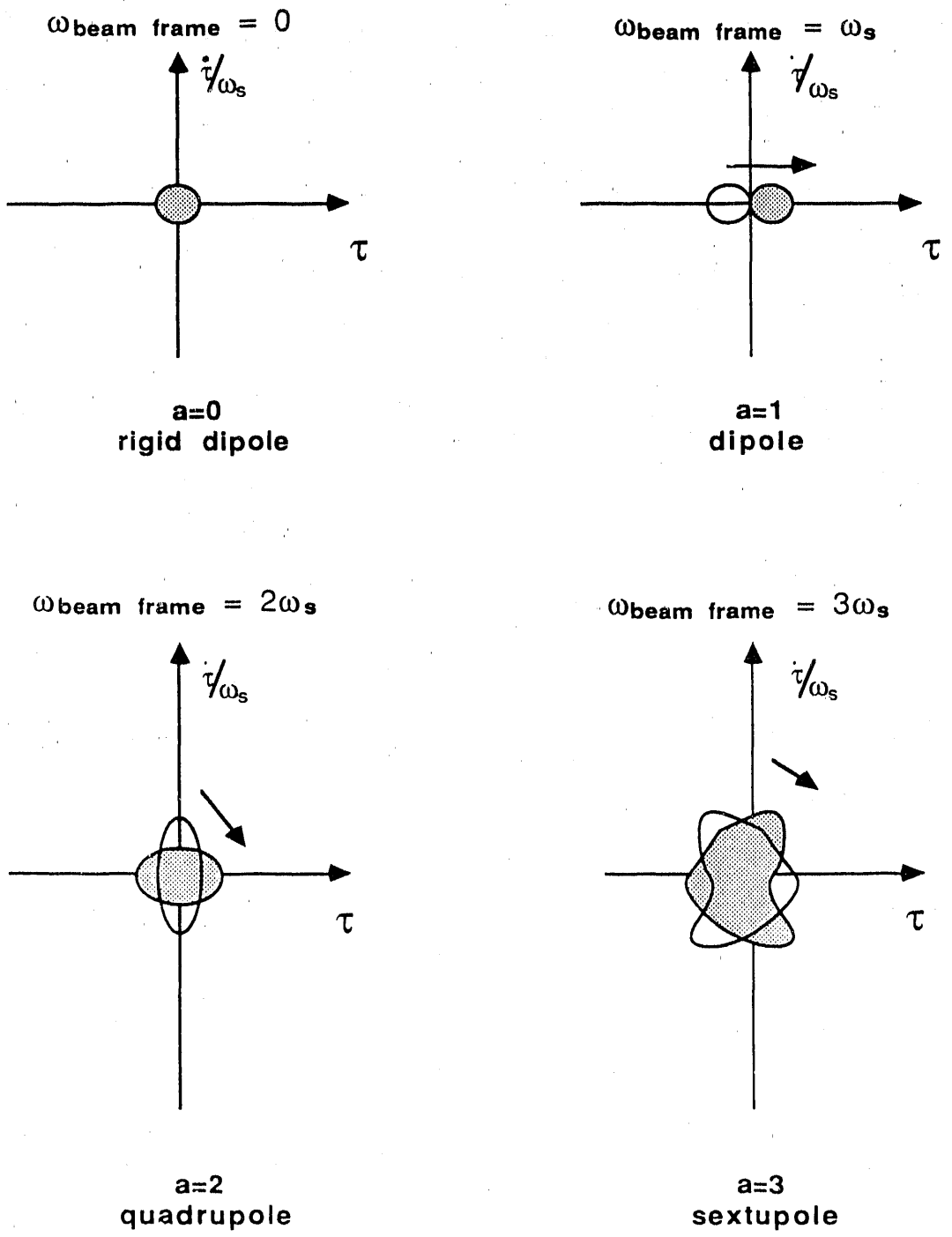

Fig. 15. Schematic diagram of coupled-bunch synchrotron modes. For the longitudinal case, the lowest mode that can give rise to an instability is the a = 1 mode, whereas for the transverse case the a = 0 mode can also be unstable.

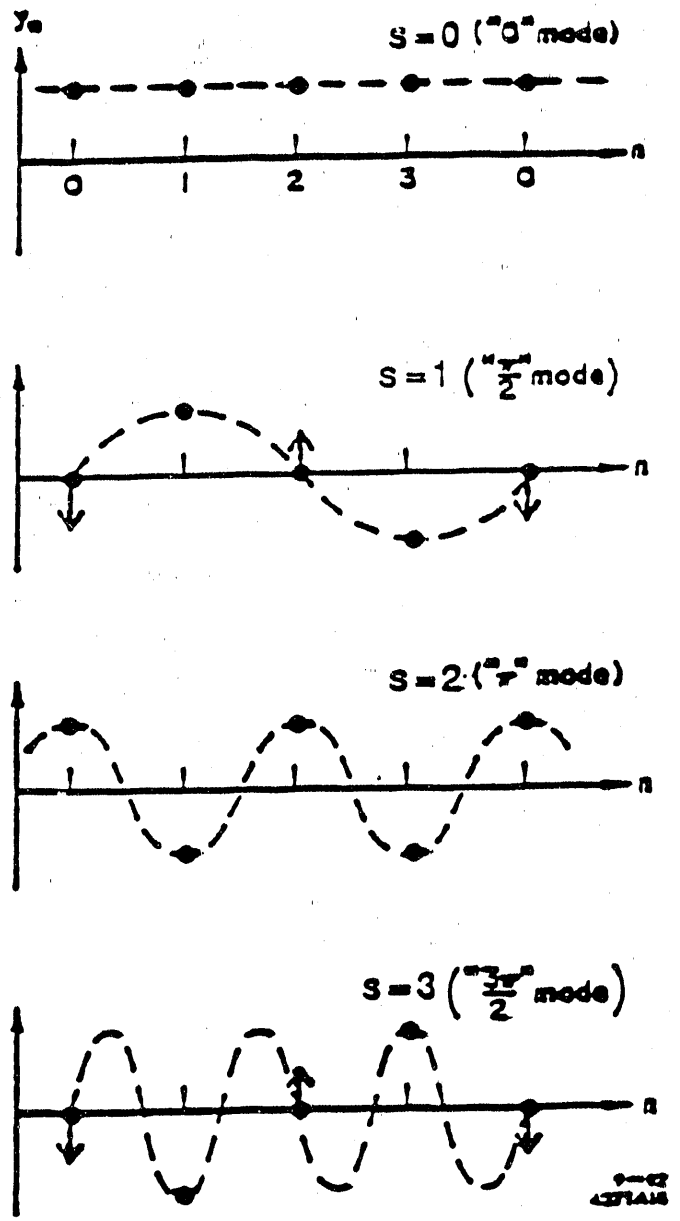

Fig. 16. Normal modes of coupled-bunch motion for the four-bunch case (taken from Ref. 10).

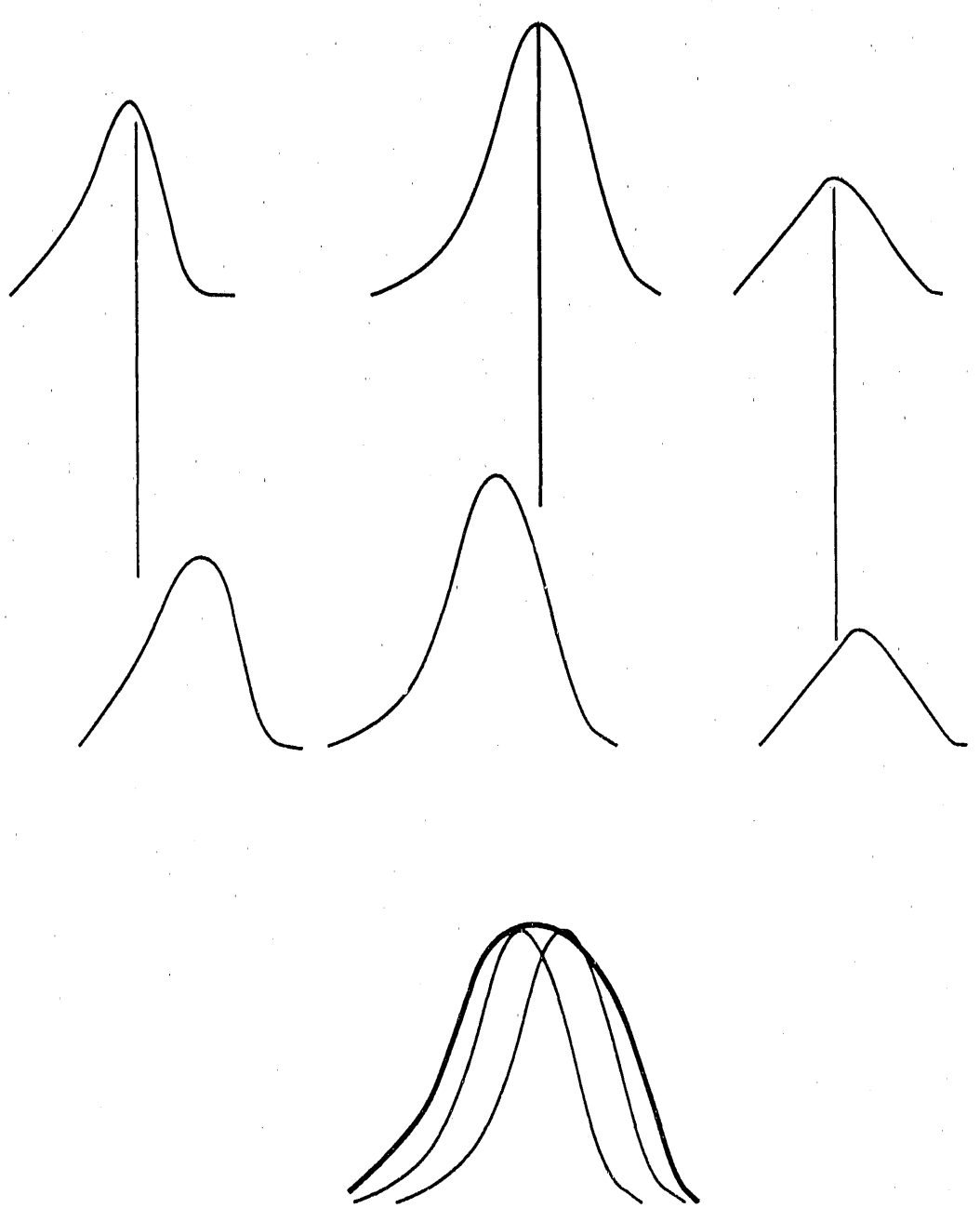

Fig. 17. Schematic picture of the de-Qing procedure to minimize calculational time.

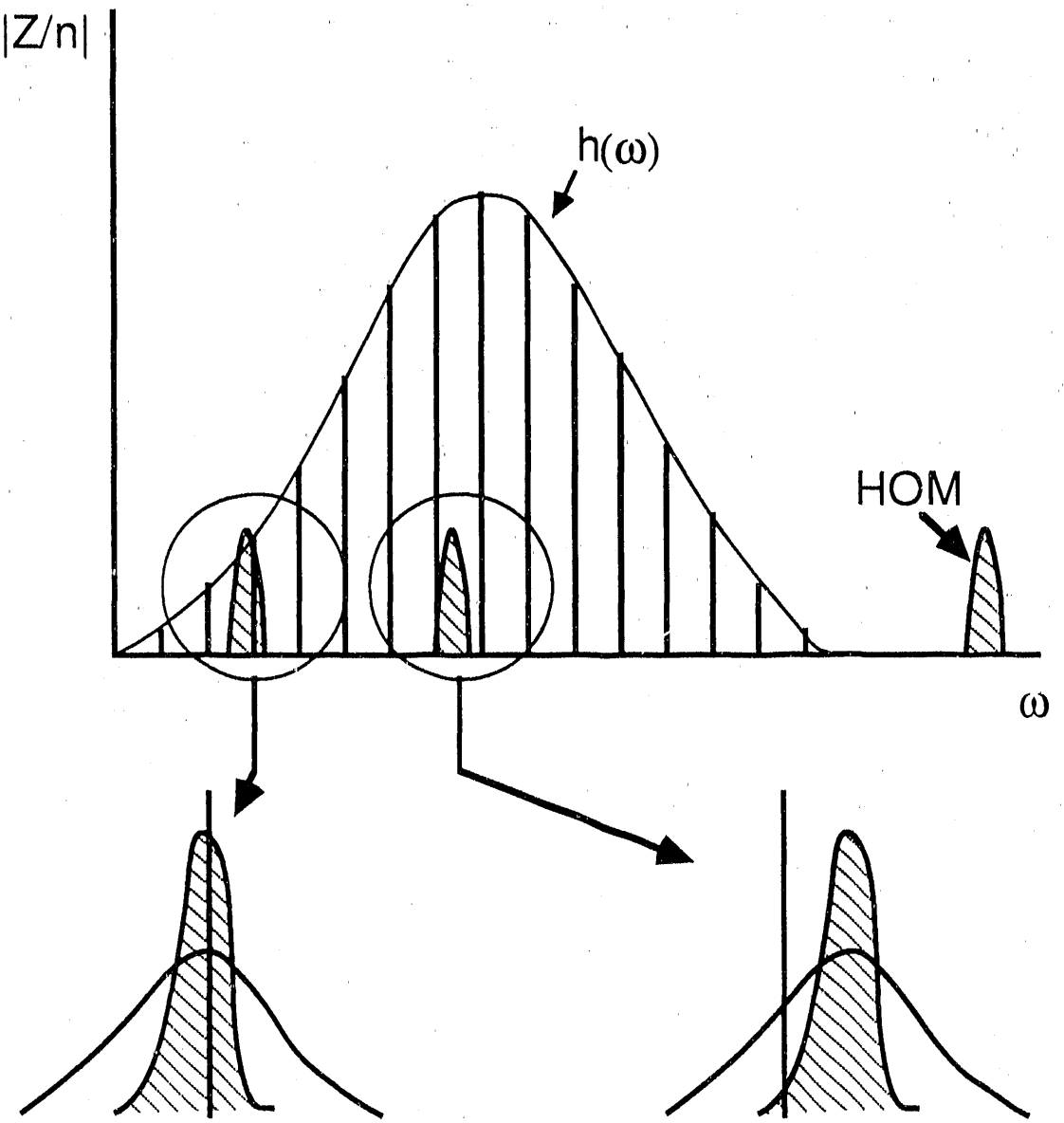

Fig. 18. Possible results of physical de-Qing of higher-order parasitic modes. If the mode is originally close to a rotation harmonic, reducing the Q will reduce the growth rate (leftmost mode). If the mode was initially between harmonics, de-Qing can give increased impedance at the rotation harmonic, and thus increased growth rate (central mode). If the higher-order mode is beyond the bunch frequency cutoff (rightmost mode), it is not sampled by the beam.

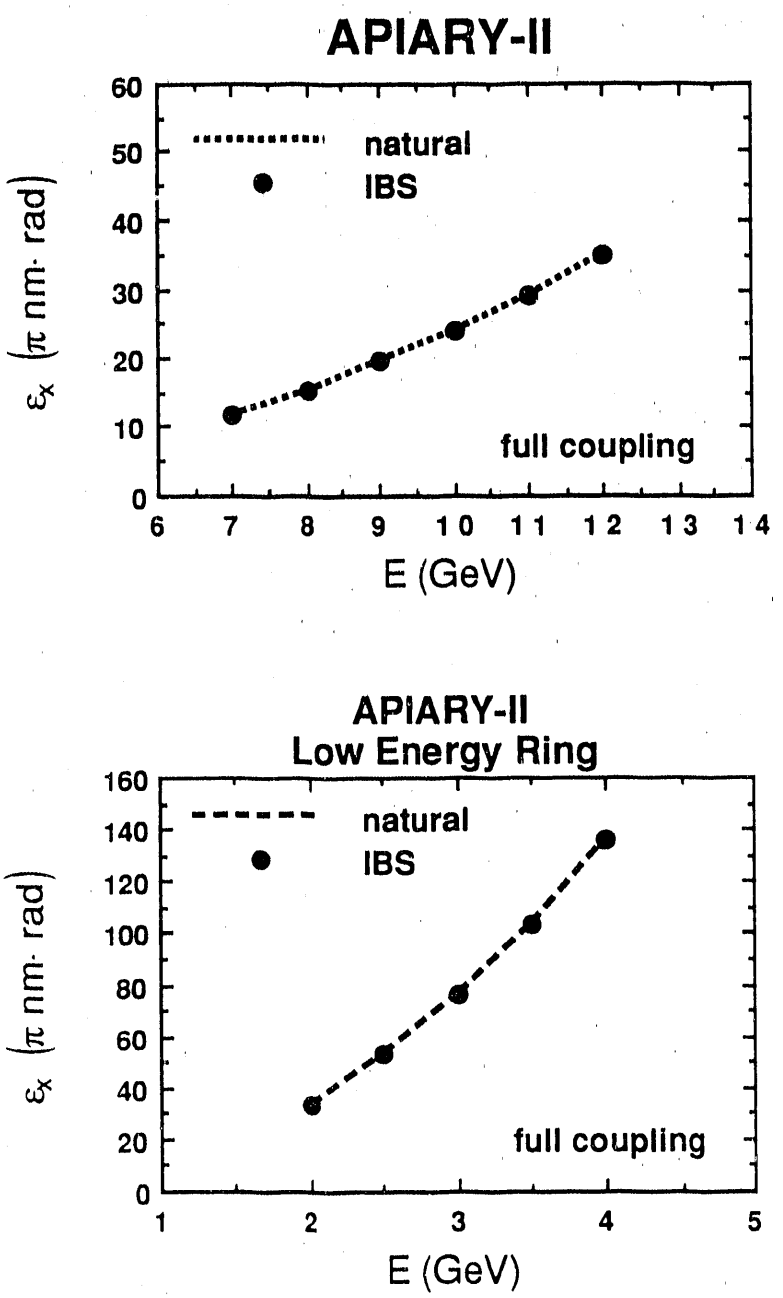

Fig. 19. Predicted emittance growth from intrabeam scattering for the B factory parameters of Ref. 14. The dots are calculated equilibrium emittance values, obtained from solving Eq. (21).

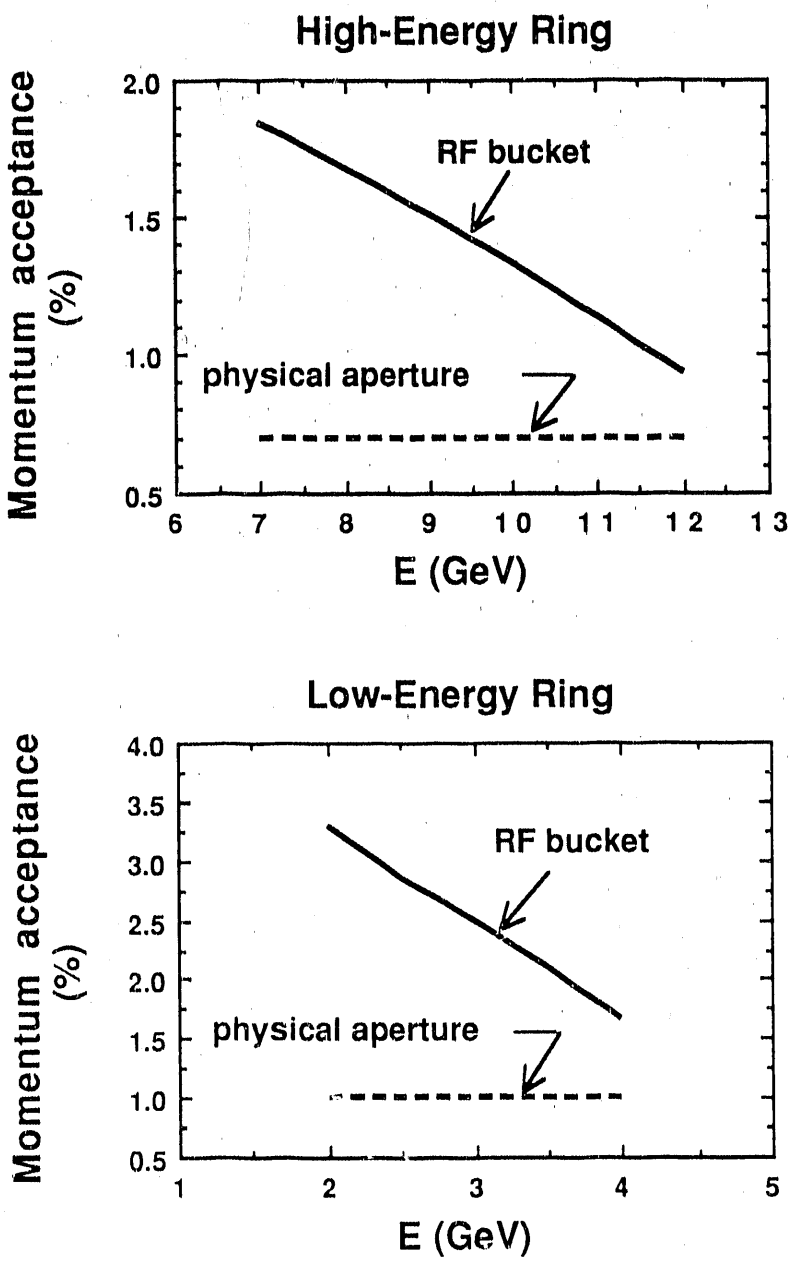

Fig. 20. Calculated momentum acceptance for the APIARY-IV rings described in Ref. 3. The transverse (physical aperture) limit is the more restrictive.

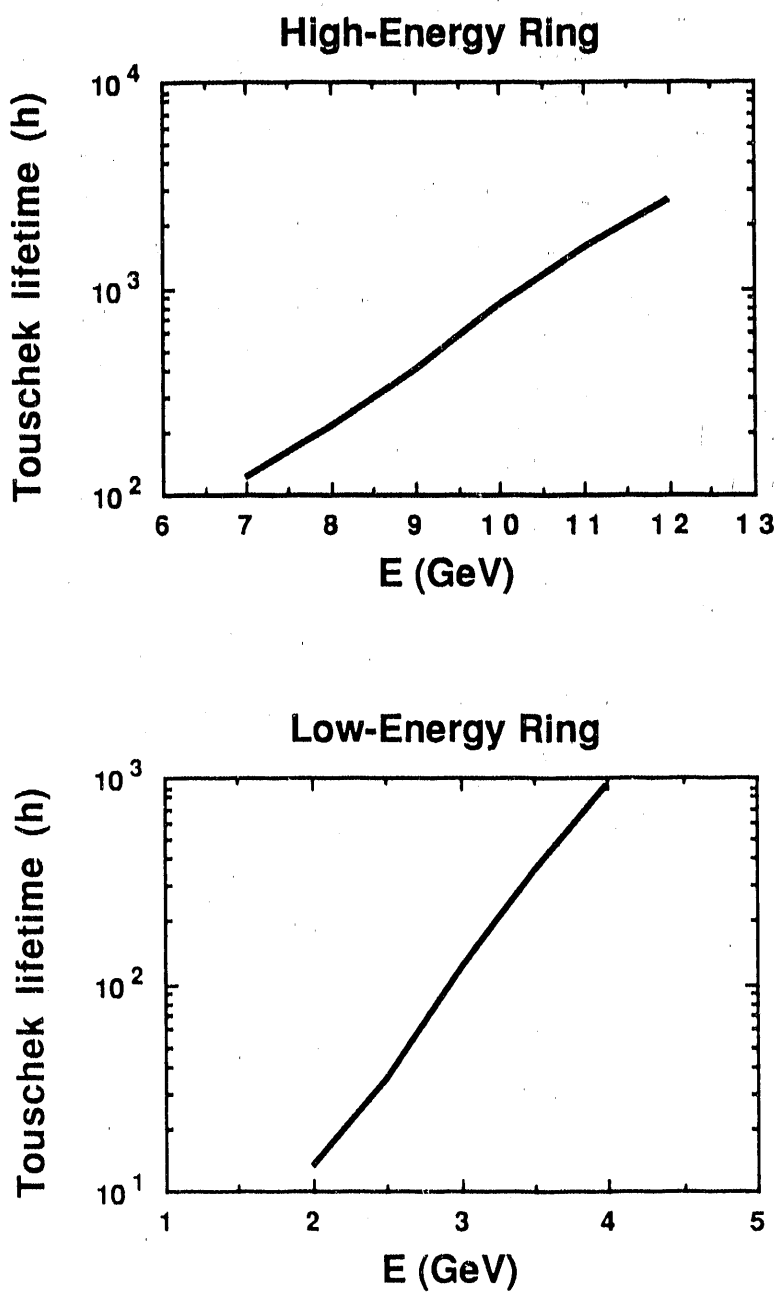

Fig. 21. Calculated Touschek lifetimes for the B factory parameters of Ref. 14.

END

DATE FILMED

11 / 26 / 90